

**UNIVERSIDAD AUTÓNOMA DE SAN LUIS POTOSÍ  
FACULTAD DE CIENCIAS QUÍMICAS**

---

**PROGRAMA DE POSGRADO EN CIENCIAS EN BIOPROCESOS**

**EFFECTO CRIOPROTECTOR Y COADYUVANTE DE LA  
MALTODEXTRINA EN LOS DIAGRAMAS DE ESTADO DE  
SISTEMAS RICOS EN AZÚCARES**

**ARTÍCULO DE INVESTIGACIÓN PARA OBTENER EL GRADO DE  
DOCTOR EN CIENCIAS EN BIOPROCESOS**

**PRESENTA:**

**M.C. FLORES RAMÍREZ ALMA DE JESÚS**

**DIRECTOR DE TESIS**

**DR. MIGUEL ANGEL RUIZ CABRERA**



EFFECTO CRIOPROTECTOR Y COADYUVANTE DE LA MALTODEXTRINA EN  
LOS DIAGRAMAS DE ESTADO DE SISTEMAS RICOS EN AZÚCARES by ALMA  
DE JESÚS FLORES RAMIREZ is licensed under a Creative Commons  
Reconocimiento-NoComercial-SinObraDerivada 4.0 Internacional  
License.

## **Proyecto realizado en:**

Laboratorio de Ingeniería en Alimentos y en el Laboratorio de Ciencia e Investigación de Alimentos de la Facultad de Ciencias Químicas de la Universidad Autónoma de San Luis Potosí.

“El programa de Maestría y Doctorado en Ciencias en Bioprocesos de la Universidad Autónoma de San Luis Potosí pertenece al Programa Nacional de Posgrados de Calidad (PNCP) del CONACYT, registro 000588 (Maestría) 000590 (Doctorado), en el Nivel Maestría (Consolidado) Doctorado (En desarrollo).

## **Agradecimientos**

Al Consejo Nacional en Ciencia y Tecnología (CONACYT) por el apoyo económico otorgado a través de la beca número 574611 brindada para la realización de mis estudios de doctorado.

Al Consejo Nacional en Ciencia y Tecnología (CONACYT) por el apoyo económico otorgado a través del proyecto CB2017-2018/A1-S-32348 y Fondo de Apoyo a la investigación UASLP con el proyecto C18-FAI-05-64-64.



**UNIVERSIDAD AUTÓNOMA DE SAN LUIS POTOSÍ  
FACULTAD DE CIENCIAS QUÍMICAS**

**PROGRAMA DE POSGRADO EN CIENCIAS EN BIOPROCESOS**

**EFFECTO CRIOPROTECTOR Y COADYUVANTE DE LA  
MALTODEXTRINA EN LOS DIAGRAMAS DE ESTADO DE  
SISTEMAS RICOS EN AZÚCARES**

**ARTÍCULO DE INVESTIGACIÓN PARA OBTENER EL GRADO DE  
DOCTOR EN CIENCIAS EN BIOPROCESOS**

**PRESENTA:**

**M.C. FLORES RAMÍREZ ALMA DE JESÚS**

**SINODALES:**

**PRESIDENTE:**

**DR. MIGUEL ANGEL RUIZ CABRERA**

**SECRETARIO:**

**DR. JAIME DAVID PÉREZ MARTÍNEZ**

**VOCAL:**

**DRA. ALICIA GRAJALES LAGUNES**

**VOCAL:**

**DR. RAÚL GONZÁLEZ GARCÍA**

**VOCAL EXTERNO:**

**DR. MIGUEL ABUD ARCHILA**

\_\_\_\_\_

\_\_\_\_\_

\_\_\_\_\_

\_\_\_\_\_

\_\_\_\_\_



San Luis potosí, Noviembre/30/2021

**Comité Académico**  
**Programa de Posgrado en Ciencias en Bioprocesos**  
**Facultad de Ciencias Químicas**  
**Universidad Autónoma de San Luis Potosí**

**Con atención a la Dra. Ruth Elena Soria Guerra**  
**Coordinadora del Programa de Posgrado en Ciencias en Bioprocesos**  
**FCQ-UASLP**  
**Presente**

Por medio de la presente hacemos de su conocimiento que la tesis llevada a cabo por la **M.C Alma de Jesús Flores Ramírez**, titulada **“Efecto crioprotector y coadyuvante de la maltodextrina sobre los diagramas de estado de sistemas ricos en azúcares”**, ha sido concluida y aprobada por el comité tutorial para dar inicio a los trámites correspondientes para su titulación, el cual tendrá lugar el día 14 de diciembre a las 11:00 horas en el Auditorio G203 de la Facultad de Ciencias Químicas.

**ATENTAMENTE**

**Comité tutorial**

Dra. Alicia Grajales Lagunes

Dr. Jaime David Pérez Martínez

Dr. Raúl González García

Dr. Miguel Abud Archila

[www.uaslp.mx](http://www.uaslp.mx)

Dr. Miguel Angel Ruiz Cabrera

## **AGRADECIMIENTOS ACADÉMICOS**

*A lo largo del desarrollo de este proyecto he tenido el apoyo de mi director de tesis, el Dr. Miguel Ángel Ruiz Cabrera, quien me ha dado las herramientas para finalizar satisfactoriamente este trabajo, además de ayudarme a desarrollar diversas capacidades que hasta el momento creía no poseer, favoreciendo mi crecimiento tanto académico como personal.*

*A las personas que forman parte del Laboratorio de Ingeniería de Alimentos de la Facultad de Ciencias Químicas de la UASLP, especialmente a la Técnico Cecilia Rivera Bautista, por brindarme su apoyo, conocimiento y consejos durante el tiempo de realización de este proyecto.*

## **AGRADECIMIENTOS PERSONALES**

*En el crepúsculo de cualquier evento en la vida, cada ser humano es responsable de las decisiones y acciones que realiza. Sin importar los obstáculos, recovecos oscuros, tropiezos, acantilados, pero siempre hay un ángel caritativo que se lamenta de tu sufrimiento y toma un poco del peso de tus calamidades en sus manos ayudándote a lograr tu felicidad. Para mí no solo hay uno sino varios ángeles en el camino que han estado ahí. Agradezco:*

*→A Dios, por permitirme llegar a este punto, por haberme dado salud para cumplir mis metas, además de su infinita bondad y amor.*

*→A mis padres (**María y José**), por depositar su confianza en mí, por haberme ayudado en todo momento, por sus consejos, motivación constante, por mostrarme como salir adelante, por su ayuda incondicional y principalmente por su amor.*

*→A mis familiares que aun que seamos pocos siempre me han mostrado su apoyo y paciencia, principalmente a **Vero** que a pesar de no ser mi hermana me ha mostrado el amor de una.*

*→A mis amigos, por sus consejos, ayuda constante y paciencia al responder a todas mis dudas.*

*No ha sido sencillo el camino que he recorrido he perdido un soporte importante de mi vida, mi ancla, pero doy gracias a su apoyo, amor e inmensa bondad. Les agradezco y hago presente mi gran afecto hacia ustedes, mi maravillosa familia. ¡Gracias, a ti que me apoyaste sin deberla ni temerla, aprendí, Gracias!*

## ÍNDICE

ÍNDICE.....	1
RESUMEN EN EXTENSO 1 .....	2
INTRODUCCIÓN .....	2
OBJETIVO.....	3
MATERIAL Y MÉTODOS .....	4
RESULTADOS .....	5
CONCLUSIÓN .....	6
BIBLIOGRAFÍA.....	6
RESUMEN GRÁFICO 1.....	7
RESUMEN EN EXTENSO 2 .....	19
INTRODUCCIÓN .....	19
OBJETIVOS.....	20
MATERIALES Y MÉTODOS.....	20
RESULTADOS .....	21
CONCLUSIÓN .....	22
BIBLIOGRAFÍA.....	23
RESUMEN GRÁFICO 2.....	24
RESUMEN EN EXTENSO 3 .....	38
INTRODUCCIÓN .....	39
OBJETIVOS.....	39
MATERIALES Y MÉTODOS.....	40
RESULTADOS .....	41
CONCLUSIÓN .....	42
RESUMEN GRÁFICO 3.....	44
CONCLUSIONES GENERALES .....	55



## **RESUMEN EN EXTENSO 1**

### **Freeze-Concentrated Phase and State Transition Temperatures of Mixtures of Low and High Molecular Weight Cryoprotectants**

#### **INTRODUCCIÓN**

La congelación y el almacenamiento en congelado se utilizan ampliamente para la conservación a largo plazo de los alimentos. Durante la congelación, la temperatura de los alimentos se disminuye para promover la formación total o parcial de los cristales de hielo, reduciendo la disponibilidad de la disponibilidad del agua así como el crecimiento microbiano y la actividad enzimática (James & James, 2014). Sin embargo, la migración de la humedad y la recristalización del hielo, inducen daños celulares y/o estructurales en los alimentos. Estos daños estructurales generalmente se manifiestan con la liberación de líquidos intracelulares, cambios en la textura y pérdida por goteo (Berk, 2009). Es importante remarcar que la intensidad del daño de la congelación depende de la composición y estructura biológica del alimento. Otro de los parámetros a considerar durante la congelación es la velocidad de congelación es la que determina el tipo, tamaño y distribución del hielo en la matriz alimenticia. Como regla general se tiene establecido que velocidades bajas de enfriamiento tienden a producir cristales grandes de hielo extracelulares mientras que la congelación rápida genera pequeños cristales de hielo uniformemente distribuidos dentro y fuera de la célula. Sin embargo, el efecto benéfico de la congelación rápida en la calidad de alimentos sigue siendo un punto de controversia porque ha sido encontrado que, aunque estos hayan sido adecuadamente congelados mediante congelación rápida, los fenómenos de recristalización durante el almacenamiento siguen presentándose. Lo anterior es debido a que no toda el agua presente en el alimento está debidamente congelada a la temperatura estándar de  $-18^{\circ}\text{C}$  (Nesvadba, 2008). Por ello, es necesario el control de la temperatura de almacenamiento a lo largo de la cadena de frío. La calidad de los alimentos

congelados se ve afectada por la temperatura de almacenamiento y el estado físico de la fase descongelada (Charoenrein & Harnkarnsujarit, 2017). Las temperaturas asociadas a la fracción máximamente crioconcentrada ( $T_m'$  y  $T_g'$ ) se consideran como parámetros de referencia que determinan la estabilidad de los alimentos congelados, asumiendo que la formación máxima de hielo tiene lugar cuando los sistemas alimentarios se almacenan entre estas temperatura (Charoenrein & Harnkarnsujarit, 2017; Zaritsky, 2018) Por debajo de  $T_g'$ , la matriz crio-concentrada alcanza el estado vítreo donde el movimiento molecular se hace extremadamente lento y cualquier cristalización de hielo se vuelve prácticamente imposible y por lo tanto se puede esperar estabilidad del alimento a largo plazo. Sin embargo, la mayoría de los alimentos tienen un valor de  $T_g'$  muy por debajo de la temperatura de congelación comercial ( $-18^{\circ}\text{C}$ ). En este contexto, el uso de crioprotectores de alto peso molecular, como la maltodextrina 4-7 DE, povidexrosa e hidrocoloides, para manipular el estado físico y elevar deliberadamente los valores de  $T_g'$  y  $T_m'$  de alimentos congelados por encima de la temperatura normal de almacenamiento de los congeladores comerciales puede ser una alternativa atractiva. Sin embargo protocolos de incorporación de compuestos crioprotectores a alimentos no han sido establecidos hasta el momento. Los factores de selección de estos solutos se han basado principalmente en su bajo costo, disponibilidad, características sensoriales agradables o aceptación en los alimentos, proceso de prueba y error así como de la experiencia de los fabricantes de alimentos. Por lo tanto se propone que la selección y rango de concentración del crioprotector sea en función de los valores  $T_g'$  y  $T_m'$ .

## **OBJETIVO**

1. Determinar las temperaturas características de la matriz máximamente crioconcentrada ( $T_g'$ ,  $T_m'$ ) y el punto de congelación ( $T_m$ ) de crioprotectores a diferentes concentraciones mediante DSC con la finalidad de establecer la concentración y tipo (s) de crioprotector.

## MATERIAL Y MÉTODOS

Maltodextrina 4 DE (M), glucosa (G), y povidona (P) grado reactivo fueron utilizadas como sustancias crioprotectoras, las cuales, fueron equilibradas sobre Drierite® con una actividad de agua ( $a_w$ ) de 0 a temperatura ambiente por un periodo de 4 semanas. Las fracciones másicas  $X_M$ ,  $X_G$ ,  $X_P$  y  $X_W$  fueron establecidas usando un diseño experimental Distance-Based para mezclas de 4 componentes sujetos a las siguientes restricciones:  $\sum_{i=1}^n X_i = 1$  y  $0.4 \leq \{X_W\} \leq 0.95$ . Un total de 30 soluciones crioprotectoras fueron preparadas en viales de 1.5 ml mediante la adición directa de  $X_W$  para lograr un volumen de 1 ml. Alícuotas de 5-10  $\mu$ l fueron tomadas de cada solución y fueron colocadas en charolas DSC (TA Instruments), las cuales fueron selladas herméticamente y se dejaron en equilibrio durante 7 días. Todos los análisis térmicos fueron realizados en un Calorímetro Diferencial de Barrido (DSC Q2000 (TA Instruments)). Las muestras fueron sometidas a un método de escaneo convencional lineal el cual consistió en un enfriamiento a  $-70^\circ\text{C}$  a una velocidad de  $20^\circ\text{C}/\text{min}$ , esta temperatura se mantuvo durante 3 min, y posteriormente fueron calentadas hasta  $20^\circ\text{C}$  a  $10^\circ\text{C}/\text{min}$ . Para muestras con una humedad de 40-60 % (b.h.) fue requerido un procedimiento de annealing a  $T_m'-1^\circ\text{C}$  con el fin de maximizar la formación de hielo. Mientras que para muestras con  $X_M$  predominante, fue necesario someter las muestras a un calentamiento desde la temperatura ambiente hasta  $80^\circ\text{C}$  a  $20^\circ\text{C}/\text{min}$  para posteriormente continuar con el escaneo lineal convencional, este procedimiento se realizó con la finalidad de lograr una completa homogenización de los componentes. Los valores de  $T_g'$  y  $T_m'$  fueron respectivamente asignados al punto medio del 1° y 2° paso de cambio de flujo de calor observados en los termogramas durante el calentamiento. La temperatura máxima correspondiente a la endoterma de fusión fue considerada como el punto de congelación ( $T_m$ ). Un modelo cúbico de Scheffe fue usado para evaluar el efecto de la composición de las mezclas crioprotectoras  $\{X_M, X_G, X_P\}$  disueltas en una fracción másica de agua ( $X_W$ ) sobre las variables de respuesta ( $T_g'$ ,  $T_m'$  y  $T_m$ ). Un análisis de

varianza (ANOVA) a un nivel de confianza de 95% ( $p < 0,05$ ), el software Design-Expert<sup>®</sup> fue utilizado.

## RESULTADOS

Los termogramas DSC de las soluciones crioprotectores revelaron la existencia de una transición vítrea para las soluciones de maltodextrina pura y dos transiciones para todas las demás soluciones. Las soluciones de maltodextrina pura mostraron valores más altos de  $T_g'$ ,  $T_m'$  y  $T_m$  (-6.3, 6.3 y 0.5°C) que los obtenidos para las soluciones congeladas de polidextrosa (-34.6, -22.6 y -7.3°C) y glucosa (-54.3, -38.2 y -15.6°C). Con el mismo contenido de humedad, esto se puede atribuir al mayor peso molecular de las maltodextrina DE 4. Estos resultados concuerdan con lo reportado en la literatura donde se han reportado que compuestos con alto peso molecular, presentan mayores valores de  $T_g'$  y  $T_m'$  y  $T_m$ .

Se pudo observar en muestras ternaria acondicionadas a humedades de 40-95%, que el aumento de la concentración de las soluciones crioprotectores aumento la intensidad de las transiciones térmicas. En todos los contenidos de humedad, las mezclas ternarias exhiben transiciones globales bien definidas, indicando una buena compatibilidad de los crioprotectores.

Ningún aumento sinérgico de  $T_g'$ ,  $T_m'$  y  $T_m$  se encontraron cuando se analizaron mezclas de crioprotectores de alto y bajo peso molecular. Los valores más alto de  $T_g'$ ,  $T_m'$  y  $T_m'$  se encontraron para soluciones de maltodextrina al 40% de agua. Por otra parte, soluciones de glucosa 40% de agua presentaron los valores más bajos de  $T_g'$ ,  $T_m'$  y  $T_m'$ . Las soluciones crioprotectores restantes presentaron valores intermedios de acuerdo a lo que se ha publicado en literatura en relación a que las mezclas de biopolímeros compatibles exhiben temperaturas de transición de fase y estado intermedias por que los componentes de las mezclas actúan como plastificantes mutuos.

Los valores experimentales de  $T_g'$ ,  $T_m'$  y  $T_m'$  obtenidos y los modelos matemáticos propuestos en esta investigación pueden ser de gran ayuda para la formulación de medios crioprotectores que contienen más de dos componentes para

mejorar la estabilidad y calidad de almacenamiento de los alimentos congelados con contenido de humedad alto e intermedio y formulación modificables.

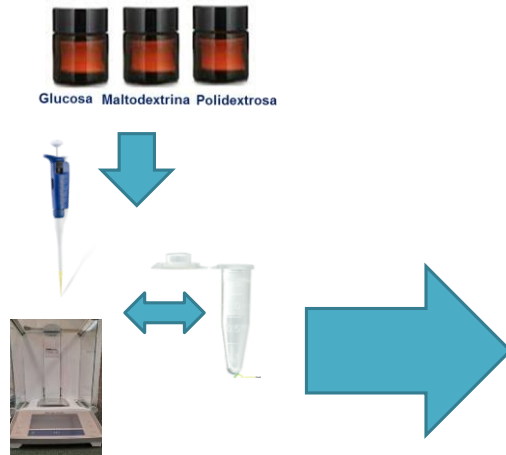
## CONCLUSIÓN

Los valores de  $T_g'$ ,  $T_m'$  y  $T_m$  aumentan con el peso molecular del crioprotector. Además, el análisis estadístico de los datos ( $p < 0.05$ ) demostró que tanto la composición del soluto como el agua deben considerarse en la formulación de medios crioprotectores, ya que se encontró que afectan significativamente los valores de  $T_g'$ ,  $T_m'$  y  $T_m$  ( $p < 0,05$ ). Las expresiones matemáticas para  $T_g'$ ,  $T_m'$  y  $T_m$  en función de las fracciones de masa de los crioprotectores ( $X_M$ ,  $X_G$ ,  $X_P$ ) y el agua ( $X_W$ ) y sus interacciones se desarrollaron para guiar la formulación de medios crioprotectores que involucran mezclas de más de dos crioprotectores para mejorar la estabilidad en almacenamiento y la calidad de productos congelados con contenidos de humedad altos e intermedia.

## BIBLIOGRAFÍA

2. Berk, Z. (2009). *Food Process Engineering and Technology*, S. L. Taylor, Ed., chapter 19, Academic Press, USA.
3. Charoenrein, S. & Harnkarnsujarit, N. (2017). *Non-Equilibrium States And Glass Transitions in Foods. Processing Effects And Product- Specific Implications*, B. Bhandari and Y. Roos, Eds., chapter 2, Woodhead Publishing, UK, 2017
4. James, S. J. & James, C. (2014). Food safety management, in *A Practical Guide for The Food Industry*, Y. Motarjemi, Ed., chapter 20, Academic Press, Bilthoven, The Netherlands.
5. Nesvadba, P., (2008). *Frozen Food Science and Technology*, J. A. Evans, Ed., chapter 1, Blackwell Publishing, Singapore.
6. Zaritzky, N. E. (2008). *Frozen Food Science And Technology*, J. A. Evans, Ed., chapter 11, Blackwell Publishing, Singapore.

# RESUMEN GRÁFICO 1

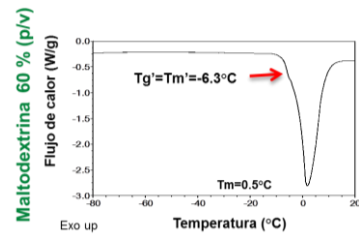


Preparación de soluciones crioprotectoras

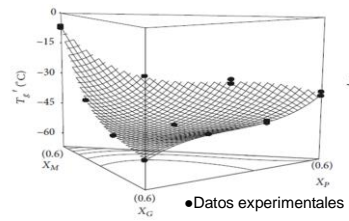


Análisis calorimétrico

Caracterización térmica de soluciones crioprotectoras



Variación de  $T_g'$  en soluciones crioprotectoras



## Research Article

# Freeze-Concentrated Phase and State Transition Temperatures of Mixtures of Low and High Molecular Weight Cryoprotectants

Alma J. Flores-Ramírez,<sup>1</sup> Pedro García-Coronado,<sup>1</sup> Alicia Grajales-Lagunes,<sup>1</sup>  
Raúl González García ,<sup>1</sup> Miguel Abud Archila,<sup>2</sup> and Miguel A. Ruiz Cabrera <sup>1</sup>

<sup>1</sup>Faculty of Chemical Science, University of San Luis Potosí, 6 Dr Manuel Nava Avenue, University Area, San Luis Potosí 78210, Mexico

<sup>2</sup>National Institute of Technology of Mexico, Technological Institute of Tuxtla Gutiérrez, Street Km 1080, Tuxtla Gutiérrez 29050, Mexico

Correspondence should be addressed to Miguel A. Ruiz Cabrera; [mruiz@uaslp.mx](mailto:mruiz@uaslp.mx)

Received 29 October 2018; Revised 1 January 2019; Accepted 10 January 2019; Published 14 February 2019

Academic Editor: Yohei Kotsuchibashi

Copyright © 2019 Alma J. Flores-Ramírez et al. This is an open access article distributed under the Creative Commons Attribution License, which permits unrestricted use, distribution, and reproduction in any medium, provided the original work is properly cited.

Although numerous studies have been conducted on the use of cryoprotectants to prevent the deterioration of food during freezing and frozen storage, scarce reports exist on the thermal transition properties of aqueous cryoprotectant solutions at frozen temperatures. The selection of a suitable cryoprotective medium for the long-term preservation of food requires knowledge of the effects of cryoprotectants and their concentration on the freeze-concentrated unfrozen phase and state transition temperatures known as  $T_g'$ ,  $T_m'$ , and  $T_m$ . Calorimetric measurements were conducted to determine the  $T_g'$ ,  $T_m'$ , and  $T_m$  values of thirty frozen aqueous solutions containing maltodextrin, polydextrose, and glucose, in which a distance-based experimental design was used for mixtures of four components to establish their corresponding mass fractions in the mixtures. Thermograms, measured during heating/rewarming from  $-70$  to  $20^\circ\text{C}$ , were used to identify the glass transition and freezing temperatures. Mathematical expressions for  $T_g'$ ,  $T_m'$ , and  $T_m$  as a function of the mass fractions of cryoprotectants and water and their interactions ( $p < 0.05$ ) were developed to aid the formulation of cryoprotective media involving more than two cryoprotectants for adequate frozen conservation of high and intermediate moisture foodstuffs.

## 1. Introduction

Freezing and frozen storage are widely used for the long-term preservation of food. During freezing, the temperature of the food is lowered to promote the total or partial formation of ice crystals, reducing the availability of water and consequently the growth of microorganisms and enzymatic activity [1–4]. Frozen foods have an extended shelf-life of months compared to days or weeks for chilled or refrigerated foods [5, 6]. Additionally, frozen foods are preferred by consumers because freeze preservation ensures that the food products present better taste, texture, nutritional value, and freshness than those preserved by other methods such as dehydration, concentration, and pasteurization [2].

However, some negative changes in frozen foods caused by physical, chemical, and/or biochemical processes resulting from inadequate freezing rates or storage temperature need

to be considered. The major physical change in frozen foods is moisture migration, which causes moisture loss by sublimation, moisture mobility and redistribution in food components, recrystallization of ice, and drip losses in thawed products [7]. It has also been noted that slow-freezing rates during freezing produce extracellular, large, sharp ice crystals, which cause water migration from the cells due to osmotic effects and subsequently lead to cellular dehydration and structural damage [3, 8–11]. On the other hand, among the various chemical changes that take place during freezing and frozen storage are lipid hydrolysis and oxidation, protein denaturation and oxidation, degradation of vitamins, and flavor changes [12].

To alleviate or moderate the deterioration of frozen foods, quick freezing involving the addition of cryoprotectants and phase/state transition concepts have been investigated [13–16]. Quick freezing rates promote the equilibrated formation

of small crystals inside and outside the products. Quick freezing, however, is only suitable for small samples and although fast freezing promotes the formation of small crystals inside the products, during frozen storage at the standard commercial freezing temperature of  $-18^{\circ}\text{C}$ , ice crystals undergo metamorphic changes, thus reducing the advantages of fast freezing [1]. This phenomenon occurs because, at  $-18^{\circ}\text{C}$ , foods exhibit an unfrozen phase in rubbery state, where mobility of unfrozen water may occur [17]. In addition, the small ice crystals formed under fast freezing conditions are thermodynamically unstable because of their high free energy, so they tend to combine with larger, more stable ice crystals during storage [2, 17]. Therefore, the stability and quality of frozen foods are significantly influenced by the storage temperature and physical state of the unfrozen phase [12, 18, 19].

The temperatures associated with the freeze-concentrated unfrozen phase ( $T_m'$  and  $T_g'$ ) are regarded as reference parameters determining the stability of frozen foods. It is assumed that maximum ice formation takes place when food systems are stored between these temperatures [12, 18–20]. It is also known that the unfrozen phase below  $T_g'$  leads to a glassy state with substantially increased viscosity (around  $10^{10}$ – $10^{12}$  Pa s), in which molecular motion becomes extremely low, and further crystallization of water into ice and chemical reactions associated with the molecular diffusion of water and other reactants are greatly reduced; therefore, long-term stability may be expected [13, 14, 17, 21–25]. However, the foods in this state are defined as nonequilibrium, metastable, amorphous, disordered materials exhibiting higher free volumes and energy levels than those of crystalline states. Therefore, some factors such as water sorption and temperature changes above  $T_g'$  will accelerate the molecular mobility related to chemical and physical changes in glassy frozen foods [12, 13, 19].

In the literature, it has been reported that  $T_m'$  and  $T_g'$  values exhibit slight variations with the water or solid content but, as a general trend, both parameters depend strongly on the type and molecular weight of the food components [20, 26–28]. Typically, it has been found that the  $T_m'$  and  $T_g'$  of homologous amorphous polymers such as maltodextrins decrease with the decreasing average molecular weight or increasing amount of plasticizer or moisture content [29–31]. For instance,  $T_g'$  values ranging from  $-15$  to  $-43^{\circ}\text{C}$  and  $T_m'$  values from  $-11$  to  $-28^{\circ}\text{C}$  have been reported for frozen solutions elaborated with 40% maltodextrin solutions with a dextrose equivalent (DE) ranging from 5 to 36 and respective molecular weights from 3600 to 500 Da [30].

However, fresh foods usually present high water contents and chemical compositions dominated by low molecular weight (LMW) components with  $T_m'$  and  $T_g'$  values well below the standard freezing temperature of  $-18^{\circ}\text{C}$ . Thus, frozen storage between the  $T_m'$  and  $T_g'$  or below  $T_g'$  is sometimes impractical from an economic point of view [20, 32, 33]. In this context, the use of cryoprotectants with high molecular weight (HMW), such as maltodextrin 5 DE, polydextrose, and hydrocolloids, to manipulate the physical state and deliberately elevate the  $T_m'$  and  $T_g'$  of

frozen foods to above the normal storage temperature of commercial freezers may be an attractive alternative [13, 34–36]. Another approach is the use of LMW cryoprotectants, such as dimethyl sulfoxide, glycerol, and glucose, to depress the freezing point ( $T_m$ ) and thereby reduce the intracellular ice formation [11, 36–38]. It is important to note that a synergistic increase of  $T_g'$  was reported by Harnkarnsujarit et al. [39] for mixtures of LMW sugars (glucose and maltose) and phosphate salts such as  $\text{Na}_3\text{PO}_4$ ,  $\text{Na}_4\text{P}_2\text{O}_7$ ,  $\text{Na}_5\text{P}_3\text{O}_{10}$ ,  $\text{K}_3\text{PO}_4$ , and  $\text{K}_4\text{P}_2\text{O}_7$  as a result of intermolecular interactions between the components. However, literature reports on the resulting  $T_m'$  and  $T_g'$  values for aqueous frozen solutions containing mixtures of HMW and LMW cryoprotectants involving a large working range of water content for adequate frozen conservation of high and intermediate moisture foodstuffs, such as fruits, ice cream, purees, jams, etc., remain scarce.

On the other hand, the optimization and selection of cryoprotectants in food formulations are a challenging task because the choice of cryoprotectants is based largely on criteria such as low cost, availability, pleasant or acceptable sensory characteristics in foods, and trial-and-error processes and experience of the food manufacturers [15, 16, 40]. For instance, sucrose and sorbitol concentrations of 4–8% [15, 40], polydextrose concentrations of 1–10% [41, 42], glucose concentrations of 5–15% [43], maltodextrin concentrations of 5–35% [36, 44–46], and maltodextrin-sugars concentrations of 20% (glucose, fructose, and sucrose) [47] have been used as cryoprotectant additives. In some cases, it has been reported that low levels of sugars and sorbitol impart a sweet taste to the products [40, 41, 43]. On the other hand, maltodextrin and polydextrose are nonsweetening and have low viscosities at high solid contents with good solubility [34, 35]. It is evident that the selection of cryoprotectants and their concentration range need to be standardized based on the resulting  $T_m'$  and  $T_g'$  values rather than on other criteria previously mentioned.

Therefore, this study was based on the assumption that the selection of a cryoprotectant medium suitable for the long-term preservation of food requires knowledge of the effect of cryoprotectants and their concentration on the freeze-concentrated phase and state transition temperatures. The evaluation of the  $T_g'$ ,  $T_m'$ , and  $T_m$  values of different frozen aqueous cryoprotectant solutions elaborated with pure or combined cryoprotectants using differential scanning calorimetry (DSC) involving a large range of water contents was the main focus of this study. For this purpose, thirty aqueous solutions containing maltodextrin, polydextrose, glucose, and their mixtures in a concentration range of 40–95% water were studied.

## 2. Materials and Methods

**2.1. Preparation of Cryoprotectant Solutions.** Analytical grade maltodextrin 4–7 DE (product no. 419672; molecular weight 3600), crystalline glucose (product no. G5767; molecular weight 180.16), both from Sigma-Aldrich CO. (St. Louis, MO), and commercial food grade noncrystalline polydextrose (molecular weight 342.3) from Henan Tailijie Biotech Co.



(China) were the employed cryoprotectants. Each cryoprotectant was previously equilibrated over Drierite® (anhydrous calcium sulfate,  $a_w \approx 0$ ) in a desiccator at room temperature for several weeks in order to obtain completely dry samples. The moisture content of these equilibrated samples was then determined by the AOAC method [48] and taken into account for the preparation of solutions, as described below.

Cryoprotectant solutions were prepared gravimetrically by weighing the appropriate amount of solid material using a Mettler-Toledo microbalance (model AG245; RS232 interface; readability 0.1 mg/0.01 mg) and adding the appropriate volume of distilled water. A completely randomized distance-based experimental design for mixtures of four components was used to establish the mass fraction of maltodextrin ( $X_M$ ), glucose ( $X_G$ ), polydextrose ( $X_P$ ), and water ( $X_W$ ) in the cryoprotectant solutions. The Modde 7.0 (Umetric AB) statistical software was used for the experimental design, in which the constraints  $\sum_1^n X_i = 1$  and  $0.4 \leq X_W \leq 0.95$  were considered. Five replicate points were used and a total of 30 cryoprotectant solutions, including pure components as well as binary and ternary mixtures, were prepared (Table 1).

Solutions containing high proportions of maltodextrin were dissolved in Eppendorf safe-lock tubes placed in a water bath at a controlled temperature (40°C). In all cases, the solutions were well stirred to obtain clear solutions at room temperature and after stored at 4°C for several days to allow for equilibration of the moisture content throughout the sample [27, 33]. The solid content of the equilibrated cryoprotectant solutions was confirmed with a digital refractometer (AR 200, Leica) at room temperature.

**2.2. Phase and State Transition Analysis of Frozen Cryoprotectant Solutions.** DSC measurements were carried out using a Q2000 differential scanning calorimeter (TA Instruments, Delaware 19720, USA) with a RCS90 cooling system using ultrapure nitrogen as the purging gas at a flow rate of 50 mL/min.

Samples of the cryoprotectant solutions (approximately 5–10 mg) were weighed in aluminum pans, hermetically sealed, and then placed in the DSC instrument at room temperature; an empty pan was used as the reference. The calorimetric methodology proposed by Sablani et al. [20] and Ruiz-Cabrera et al. [33] was used for determination of the  $T_m$ ,  $T_m'$ , and  $T_g'$  values of the samples. Before starting the experiments, the samples were equilibrated in the DSC apparatus at 20°C for 2 min. The samples were then cooled to -70°C at 20°C/min to quickly reach the amorphous state, maintained at this temperature for 3 min, and then heated back to room temperature at a rate of 10°C/min. It is important to note that, for cryoprotectant solutions containing water in the range of 40% to 60% wet basis ( $0.4 \leq X_W \leq 0.6$ , Table 1), an annealing procedure at ( $T_m' - 1$ )°C for 30 min was implemented to obtain maximally freeze-concentrated cryoprotectant matrices [33, 49]. The apparent value of  $T_m'$  in each experiment was determined from the first thermal analysis in nonannealed state. In these cases, each cryoprotectant solution was cooled to -70°C, held for 3 min, heated at 10°C/min to the annealing temperature ( $T_m' - 1$ )°C, and then annealed for 30 min. Following annealing, the

samples were cooled at 20°C/min to -70°C, held for 3 min, and then reheated at 10°C/min back to room temperature. The midpoint  $T_g'$  and  $T_m'$  values were determined using the half-height method from the first and second step changes of the heat flow, as observed in the DSC thermograms during the heating process [33, 50, 51]. In this study, the peak temperature corresponding to the melting endotherm was considered to be the freezing point ( $T_m$ ). In all cases, the Universal Thermal Analysis software (version 4.4A) was used.

**2.3. Statistical Analysis of the Data.** Analysis of variance (ANOVA) was performed with a confidence level of 95% ( $\alpha = 0.05$ ) using the Modde 7.0 statistical software (Umetrics, Kinnelon, NJ, USA). The Scheffe cubic model (Eq. (1)) with interactions was used to analyze the effect of the chemical composition of the cryoprotectant solutions ( $X_M$ ,  $X_G$ ,  $X_P$ , and  $X_W$ ) on the response variables ( $T_g'$ ,  $T_m'$ , and  $T_m$ ) as follows:

$$\begin{aligned}
 Y = & a_0 X_M + a_1 X_G + a_2 X_P + a_3 X_W + a_4 X_M X_G + a_5 X_G X_P \\
 & + a_6 X_P X_W + a_7 X_M X_W + a_8 X_G X_W + a_9 X_M X_P \\
 & + a_{10} X_M X_G X_P + a_{11} X_M X_G X_W + a_{12} X_M X_P X_W \\
 & + a_{13} X_G X_P X_W + a_{14} X_M X_G (X_M - X_G) \\
 & + a_{15} X_M X_P (X_M - X_P) + a_{16} X_M X_W (X_M - X_W) \\
 & + a_{17} X_G X_P (X_G - X_P) + a_{18} X_G X_W (X_G - X_W) \\
 & + a_{19} X_P X_W (X_P - X_W)
 \end{aligned} \quad (1)$$

where  $a_0$  to  $a_{19}$  are the regression coefficients of the model. A backward elimination regression with an  $\alpha$  value of 0.10 was applied and hierarchical models were obtained from Eq. (1).

### 3. Results and Discussion

**3.1. Determination of  $T_g'$ ,  $T_m'$ , and  $T_m$  in Frozen Cryoprotectant Solutions.** The DSC thermograms showing the process of rewarming from -70 to 20°C for annealed solutions of maltodextrin (Experiment 2), polydextrose (Experiment 1), and glucose (Experiment 27), all conditioned at 40% water, are shown in Figures 1(a)–1(c). No evidence of an exothermic peak associated with the recrystallization of unfrozen water is observed in the rewarming thermograms, confirming that maximally freeze-concentrated phases were obtained after the annealing treatment at  $T_m' - 1$ °C for 30 min. Instead, the DSC thermograms show thermal events in which the endothermic peak of ice melting is the most visible feature, preceded by one or two changes in the baseline with characteristics typical of a glass transition depending on the cryoprotectant. For instance, only one transition is observed for the maltodextrin solution (Figure 1(a)), while two transitions appear for the mixtures of polydextrose and glucose (Figures 1(b)–1(c)). These results are consistent with numerous previous studies, where solutions of LMW carbohydrates, such as glucose, fructose, sucrose, and trehalose, were found to exhibit two glass transition-like thermal events, while HMW polysaccharides, such as maltodextrin and starch, exhibited

TABLE 1: Distance-based experimental design for mixture of four components and measured response variables.

Exp No.	Run orden	$X_M$	$X_G$	$X_P$	$X_W$	$T'_g$	$T'_m$	$T_m$
1	1	0	0	0.6	0.4	-34.6	-22.6	-7.3
2	26	0.6	0	0	0.4	-6.3	-6.3	0.5
3	3	0	0.6	0	0.4	-54.2	-39.2	-15.4
4	4	0.017	0.017	0.017	0.95	N.D.	N.D.	1.8
5	29	0.2	0.2	0.2	0.4	-48.5	-36.1	-15.2
6	12	0.325	0	0	0.675	-7.1	-7.1	1.0
7	8	0	0.325	0	0.675	-53.4	-30.1	-3.9
8	27	0	0	0.325	0.675	-32.7	-20.1	-0.3
9	7	0.4	0.2	0	0.4	-38.6	-18.4	-2.1
10	17	0.2	0.4	0	0.4	-49.7	-28.6	-6.2
11	16	0.4	0	0.2	0.4	-29.9	-14.9	-1.0
12	10	0.2	0	0.4	0.4	-30.1	-16.9	-1.4
13	30	0	0.4	0.2	0.4	-47.2	-28.4	-9.5
14	20	0	0.2	0.4	0.4	-44.8	-29.4	-11.3
15	28	0.108	0.108	0.108	0.675	-38.9	-24.3	-0.6
16	22	0.217	0.2	0	0.583	-40.2	-25.0	-2.5
17	14	0.217	0	0.2	0.583	-25.6	-11.5	1.5
18	24	0	0.217	0.2	0.583	-45.7	-28.1	-4.7
19	11	0.354	0.054	0.054	0.538	-23.8	-14.1	-0.4
20	25	0.054	0.354	0.054	0.538	-51.3	-36.1	-5.4
21	6	0.054	0.054	0.354	0.538	-39.2	-20.5	-2.8
22	19	0.079	0.054	0.054	0.813	-37.0	-21.1	1.1
23	21	0.154	0.154	0.154	0.538	-40.4	-27.0	-1.9
24	23	0.217	0.017	0	0.767	-23.1	-11.0	1.1
25	9	0.017	0.217	0.000	0.767	-51.7	-30.3	-1.3
26	15	0	0	0.6	0.4	-36.5	-22.5	-7.1
27	2	0	0.6	0	0.4	-54.3	-39.2	-15.6
28	5	0.6	0	0	0.4	-7.3	-7.3	1.8
29	18	0.2	0	0.4	0.4	-32.2	-14.4	-1.9
30	13	0	0.2	0.4	0.4	-45.8	-30.0	-11.9

N.D.: not detected.

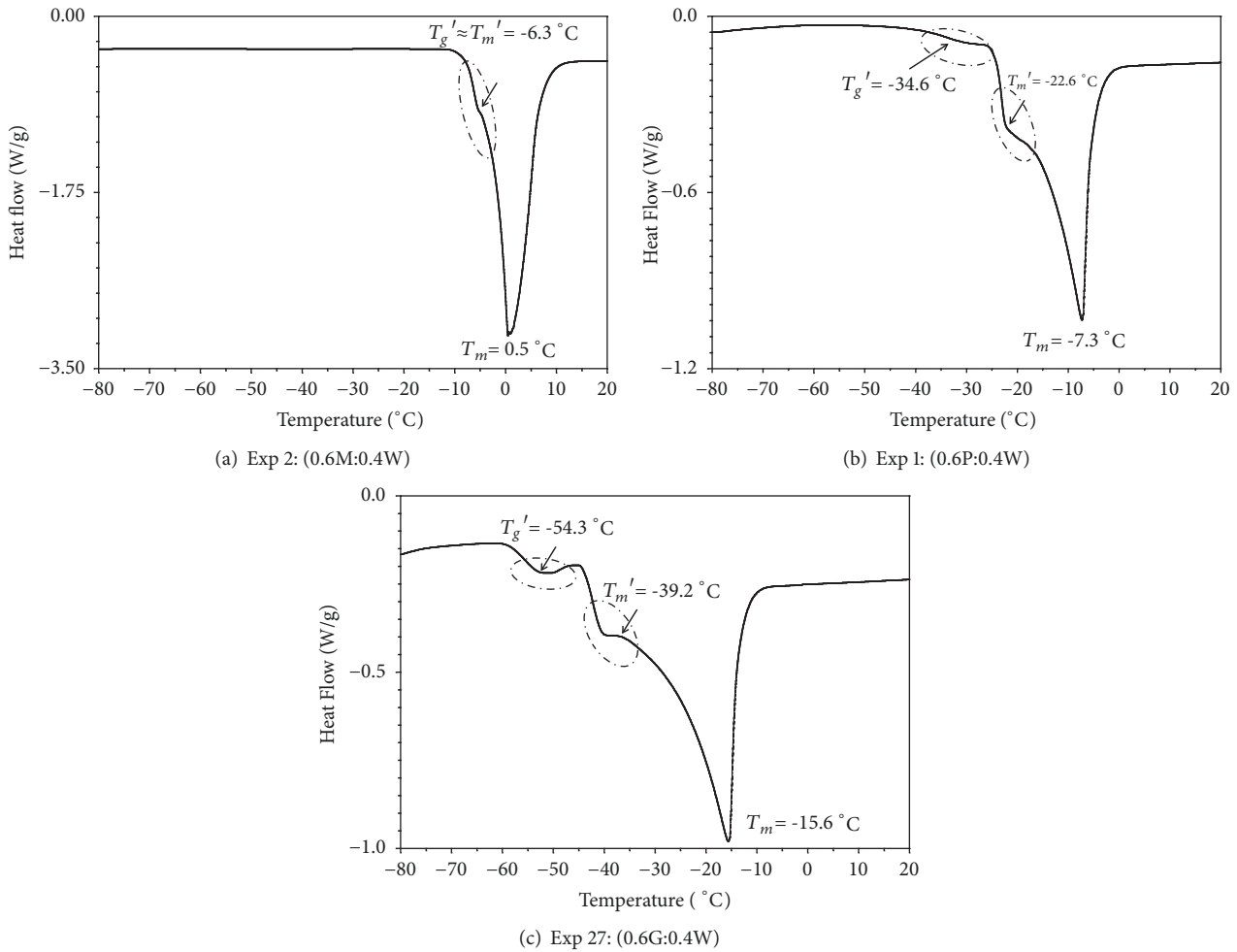


FIGURE 1: Phase and state transition analysis of frozen cryoprotectant solutions containing pure components prepared at a moisture content of 40% wet basis ( $X_W = 0.4$ ) and annealed for 30 min at  $(T_m' - 1)^\circ\text{C}$ : (a) Exp 2, (b) Exp 1, and (c) Exp 27.

a single transition by DSC analysis [20, 30, 32, 43, 51–55]. The origin of these two glass transitions is not completely understood; notions such as incompatibility of different solutes in the mixture, unequilibrated phases trapped around or within nucleated ice crystals, and reduced mobility of some components have been proposed to explain these transition events [51]. For aqueous sugar solutions, it has been suggested that the first transition can be attributed to a glass transition of the maximally freeze-concentrated phase, designated as  $T_g'$ , while the second transition can be interpreted as the beginning of the melting of ice crystals, often designated as  $T_m'$  [30, 32, 33, 50–52]. In the case of protein aqueous solutions, it has been suggested that the first transition corresponds to a glass transition of part of unfrozen water, while the second transition corresponds to a glass transition of the primary chain of the hydrated protein [32]. Thus, a similar approach to those used for sugar solutions was implemented for the determination of the  $T_g'$  and  $T_m'$  of cryoprotectant solutions.

On the other hand, it has been reported that maltodextrin solutions exhibit a broad glass transition temperature range,

attributed to its large molecular weight, and that the difference between  $T_g'$  and  $T_m'$  is likely to be very small or even null, or the glass transition may overlap with the ice melting [20, 30, 55]. For example, it has been reported by Roos and Karel [30] that the higher the molecular mass of maltodextrin, the lower the difference between the  $T_g'$  and  $T_m'$  values. However, it is probable that additional factors, such as high viscosity, ability to trap and bind water, maltodextrin-water interactions, or the amount of nonfreezable water, may be involved [56]. Thus, for practical considerations in this study, the  $T_g'$  and  $T_m'$  values were considered to be identical when solutions of maltodextrin at 40% water were used, as shown in Figure 1(a).

As shown in Figure 1, frozen solutions of pure maltodextrin (Experiment 2, Table 1) exhibited higher values of  $T_g'$ ,  $T_m'$ , and  $T_m$  ( $-6$ ,  $-6.3$  and  $0.5^\circ\text{C}$ ) than those obtained for frozen solutions of polydextrose (Experiment 1:  $-34.6$ ,  $-22.6$ , and  $-7.3^\circ\text{C}$ ) and glucose (Experiment 27:  $-54.3$ ,  $-39.2$ , and  $-15.6^\circ\text{C}$ ) at the same water content; this can be attributed to the higher molecular weight of maltodextrin. Roos and Karel [30] also reported that decreasing DE in maltodextrins

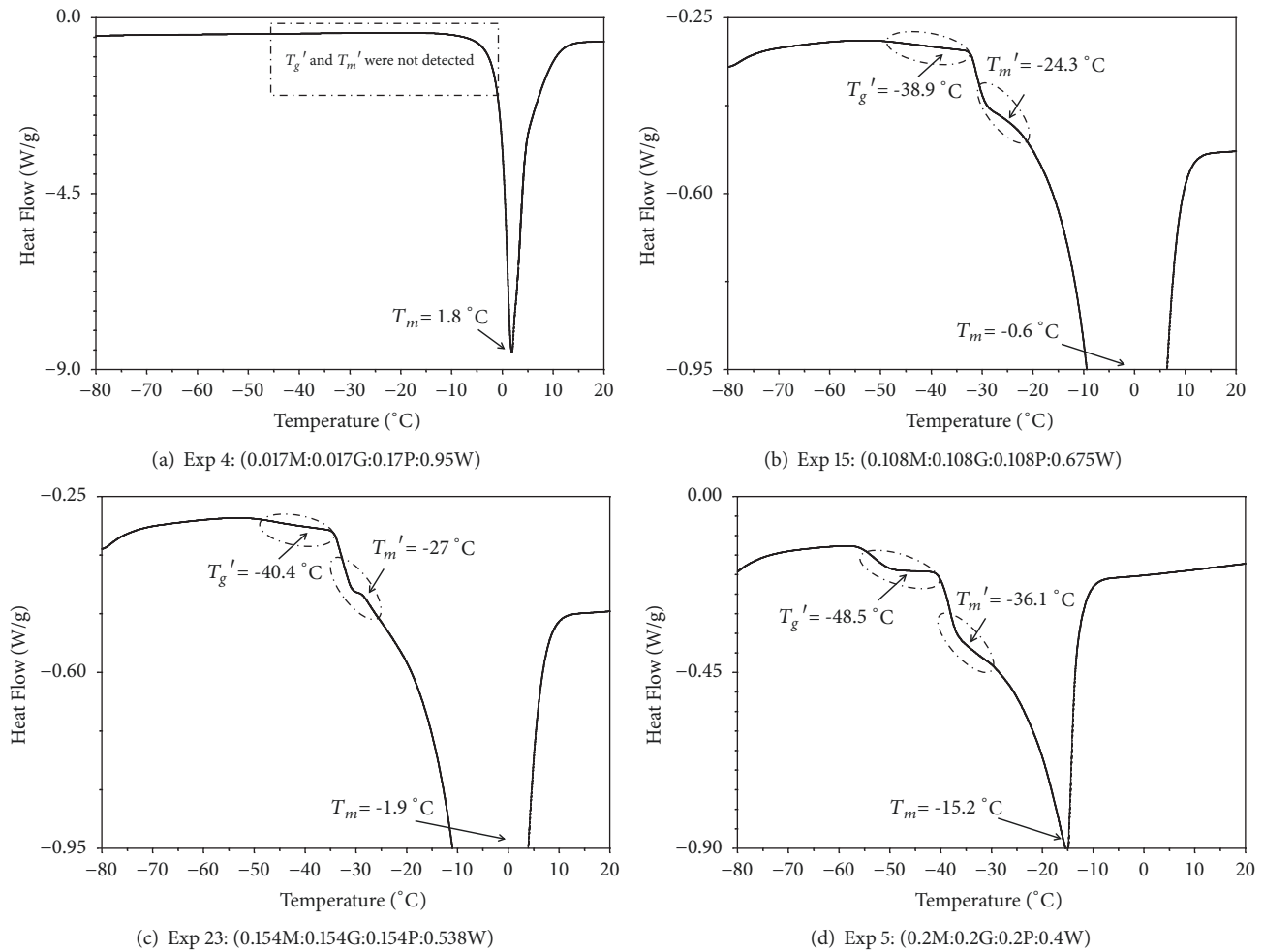


FIGURE 2: Phase and state transitions analysis of frozen ternary cryoprotectant solutions prepared at moisture contents in the range of 40–95% wet basis ( $0.4 < X_W < 0.95$ ): (a) Exp 4, (b) Exp 15, (c) Exp 23, and (d) Exp 5. Exp 23 and Exp 5 were annealed for 30 min at  $(T_m' - 1)^\circ\text{C}$ .

increased the molecular weight of the system and shifted the  $T_g'$  to a higher temperature. The  $T_g'$  and  $T_m'$  values determined for the pure maltodextrin solution prepared at 40% water are slightly higher than the values of  $T_g'$  ( $-15^\circ\text{C}$ ) and  $T_m'$  ( $-11^\circ\text{C}$ ) reported by Roos and Karel [30] when a solution of maltodextrin at 60% water with a similar DE of 5 was prepared. It is likely that the difference in the moisture content in the matrices is the main factor causing these discrepancies [12].

Typically, reports have shown that the higher the molecular weight of the cryoprotectant, the higher the  $T_g'$ ,  $T_m'$ , and  $T_m$  values. The same trend has been reported in other studies when solutions of LMW and HMW carbohydrates were used [36, 43, 55]. In general,  $T_m'$  can be increased by addition of high molecular weight compounds as a result of an increase in the viscosity of the unfrozen phase which may delay crystallization of water [30, 57]. With regard to the  $T_m$  values, based on the colligative properties of a solution, the freezing point is directly proportional to the molal concentration of the solute [37]. This indicates that the lower the molecular mass of the solute, the higher the freezing point depression,

as shown in Figure 1. Information on the freezing point depression is important for chilling and freezing processes, where reduction or inhibition of ice formation is required [3, 4].

For comparison, Figures 2(a)–2(d) show the DSC thermograms obtained for frozen ternary mixtures of cryoprotectants prepared with moisture contents in the range of 40–95% wet basis ( $0.4 < X_W < 0.95$ ). The mixture containing 95% water (Figure 2(a), Experiment 4) showed no apparent glass transition events, because only the ice-melting peak was detected during heating. It is likely that the change in heat capacity ( $\Delta C_p$ ) at the glass transition range decreased with the solid content, resulting in  $T_g'$  and  $T_m'$  values for this sample outside the limits of detection [32, 54]. However, it was noted that the increase in the concentration of cryoprotectant solutions enhanced the intensity of thermal transitions, whereby the  $T_g'$  and  $T_m'$  values could be adequately determined in Experiments 15, 23, and 5 (Figures 2(b)–2(d)). It can also be observed in Figures 2(b)–2(d) that, at all moisture contents, the ternary mixtures exhibit well-defined global transitions, indicating good compatibility of the cryoprotectants [33, 56].

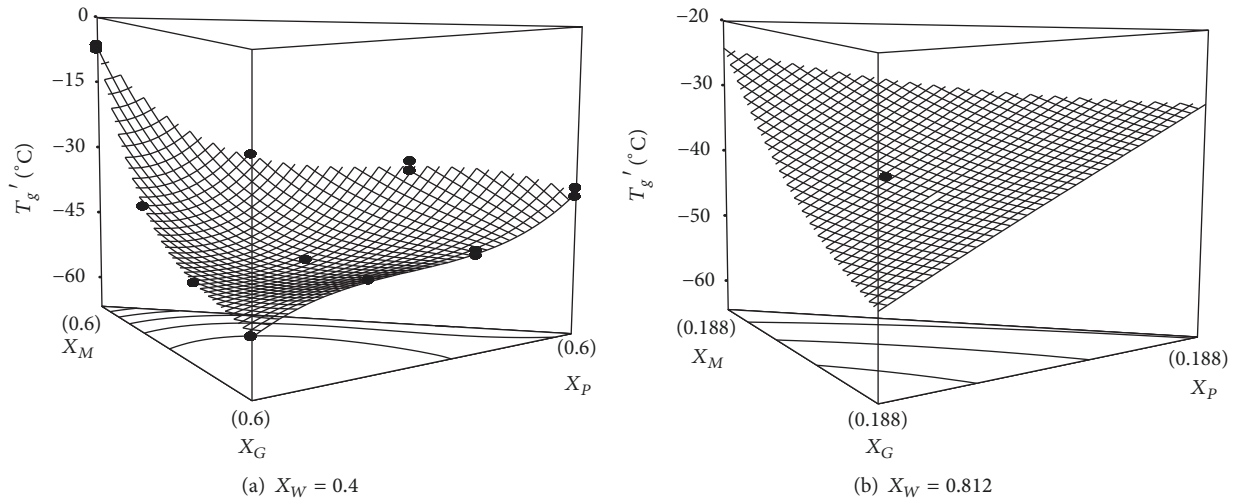


FIGURE 3: Response surface plots showing the variation of the experimental and predicted values of  $T_g'$  for different cryoprotectant solutions: (a)  $X_W = 0.4$  and (b)  $X_W = 0.812$ . ● Experimental data.

The same behavior was observed for binary-component cryoprotectant solutions (DSC thermograms not shown).

The values of  $T_g'$ ,  $T_m'$ , and  $T_m$  corresponding to each treatment are presented in Table 1. This table shows that the glass transition temperatures ( $T_g'$  and  $T_m'$ ) and freezing point ( $T_m$ ) values vary from  $-54.3$  to  $-6.3^\circ\text{C}$ ,  $-39.2$  to  $-6.3^\circ\text{C}$ , and  $-15.6$  to  $1.8^\circ\text{C}$ , respectively. In general, these values are of the same order of magnitude as those reported in studies using similar saccharide solutions [30, 43, 55, 58]. According to the data in Table 1, no synergistic increase of  $T_g'$  and  $T_m'$  was found when mixtures of HMW and LMW cryoprotectants were analyzed. From Table 1, it can be observed that the highest  $T_g'$ ,  $T_m'$ , and  $T_m$  values were found for solutions of maltodextrin at 40% water (Experiments 2 and 28) and the lowest values with solutions of glucose at 40% water (Experiments 3 and 27), with intermediate values for all the other cryoprotectant solutions. Typically, a mixture of compatible biopolymers exhibits intermediate state and phase transition temperatures because the components in the sample act as mutual plasticizers [56, 57]. Harnkarnsujarit et al. [47] had also reported that sugars such as sucrose, glucose and fructose depressed the  $T_m'$  and  $T_g'$  values of the maltodextrin-sugars systems.

**3.2. Regression Analysis and Response Surface Plots.** The uncoded regression coefficients, results of variance analysis (ANOVA), coefficients of determination ( $R^2$ ), coefficients of variation (CV%), and model significance ( $p > F$ ) obtained with (1) for  $T_g'$ ,  $T_m'$ , and  $T_m$  are presented in Table 2. From these results, it can be observed that the response variables show a high level of significance for the regression equation ( $p < 0.0001$ ), being nonsignificant for the lack of fit ( $p > 0.05$ ), indicating the effectiveness of the regression analysis. Additionally, the  $R^2$  values indicated that over 98% of the variability in the responses could be explained by the proposed models, also presented in Table 2.

According to the analysis of variance (Table 2),  $T_g'$ ,  $T_m'$ , and  $T_m$  are all primarily affected by the linear terms of the cubic model, followed by interactions between binary and ternary components. Based on the literature, it is generally accepted that the  $T_m'$  and  $T_g'$  values are independent of the initial solute concentration or moisture content. The results from some studies have indicated that  $T_g'$  and  $T_m'$  exhibit slight variations according to the moisture content and, therefore, average values have been reported for several food products [20, 26, 30, 33]. However, the results from the present study show that the moisture content of the cryoprotectant solutions ( $p < 0.0001$ , Table 2) is also a crucial factor influencing these thermal parameters.

Three-dimensional response surface plots for  $T_g'$  (Figure 3),  $T_m'$  (Figure 4), and  $T_m$  (Figure 5) using two different moisture contents for each response variable were constructed in order to gain better understanding of the interactive effects of the three cryoprotectants ( $X_M$ ,  $X_G$ ,  $X_P$ ) on the corresponding variables. The results presented in Figures 3–5 demonstrate that, in all cases, good agreement exists between the experimental and predicted values ( $R^2 > 0.98$ ). Also, the profiles in Figures 3–5 show that, at all moisture contents, the maximum glass transition and freezing temperatures appear at the points corresponding to pure maltodextrin, while the minimum values were obtained for the samples containing pure glucose. The values in good agreement with the experimental results are presented in Table 1. From the point of view of the glass transition concept, this behavior suggests that maltodextrin exhibits a greater cryostabilizing effect than polydextrose and glucose. For instance, maltodextrin DE 18 showed a higher effectiveness against lipid oxidation than an equiproportional mixture of sucrose and sorbitol in frozen-stored minced muscle of Atlantic mackerel [44]. On the other hand, Rodríguez-Furlán et al. [43] found that inulin exhibits better stabilizing properties than glucose and sucrose in the preservation of

TABLE 2: Uncoded regression coefficients and variance analysis of the hierarchical mathematical models to evaluate the variation of response variables as a function of chemical composition of the cryoprotectant solutions ( $p < 0.05$ ).

Effect	Response variables			
	$T'_g$	$T'_m$	$T_m^*$	$p > t$
	a values	a values	a values	
$X_M$	-150.42	-25.84	542.57	< 0.0001
$X_G$	-51.85	-42.15	-425.77	< 0.0001
$X_P$	109.26	-154.73	-364.76	< 0.0001
$X_W$	-50.10	-19.77	490.96	< 0.0001
$X_M X_G$	127.35	261.83	233.10	0.6304
$X_G X_P$	-61.02	111.71	-45.29	0.1788
$X_P X_W$	-272.34	279.03	777.85	0.9517
$X_M X_W$	397.90	69.14	-314.98	0.0343
$X_G X_W$	-13.08	-24.86	335.40	0.3756
$X_M X_P$	-35.29	-51.63	-3827.75	0.5986
$X_M X_G X_P$	-427.34	-1642.90	-22925.84	< 0.0001
$X_M X_G X_W$	-580.60	-672.41	-	0.0057
$X_M X_P X_W$	-369.15	345.36	10794.51	0.1057
$X_G X_P X_W$	-281.90	-	-	-
$X_M X_G (X_M - X_G)$	-156.36	-	-	-
$X_M X_P (X_M - X_P)$	-271.59	-137.14	-2310.27	0.0201
$X_M X_W (X_M - X_W)$	166.11	-	-	-
$X_G X_P (X_G - X_P)$	130.49	183.97	2801.85	0.0037
$X_G X_W (X_G - X_W)$	-	-	-	-
$X_P X_W (X_P - X_W)$	-328.21	234.05	-	0.0942
<b>Models</b>				
$p > F$	< 0.0001	< 0.0001	< 0.0001	< 0.0001
$R^2$	0.9971	0.9907	0.9849	0.9849
Lack of fit	0.2205	0.1066	0.2302	0.2302
C.V. (%)	3.38	5.90	8.57	8.57

\* Note: according to a Box-Cox analysis, a transformation  $Tm^* = (Tm + 20)^2$  on  $Tm$  values was carried out to stabilize the variance.



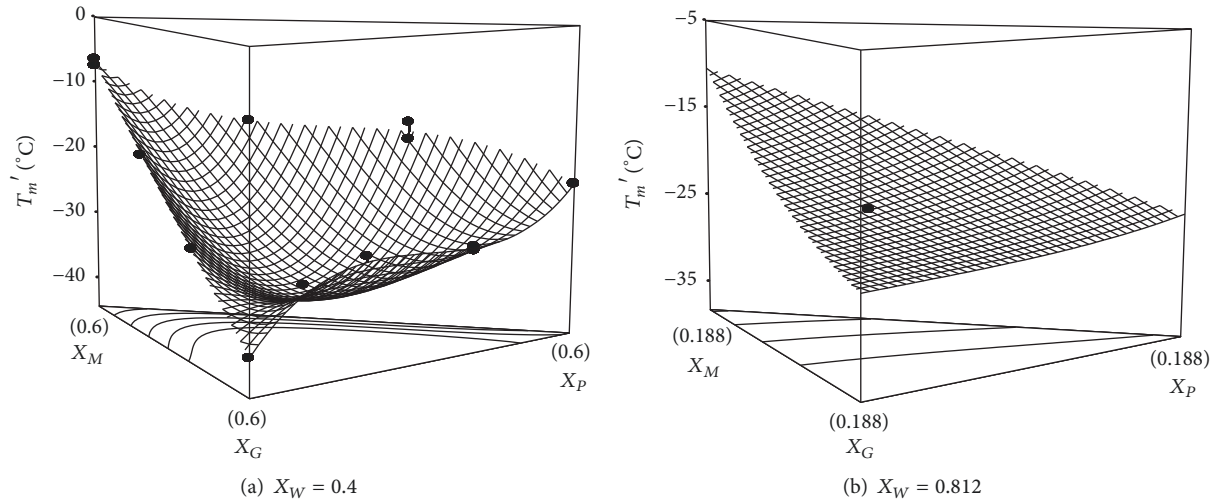


FIGURE 4: Response surface plots showing the variation of the experimental and predicted values of  $T_m'$  for different cryoprotectant solutions: (a)  $X_W = 0.4$  and (b)  $X_W = 0.812$ . ● Experimental data.

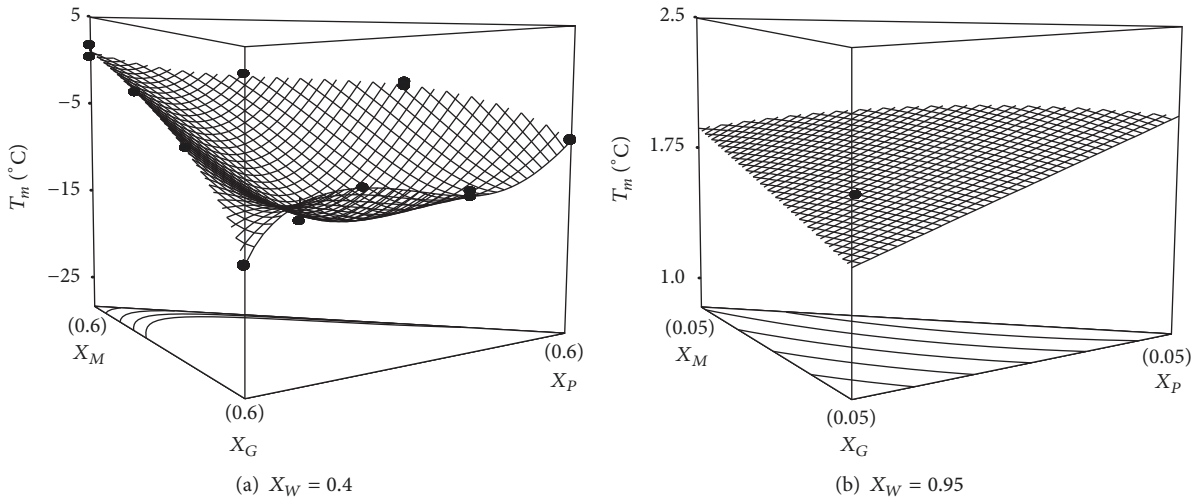


FIGURE 5: Response surface plots showing the variation of the experimental and predicted values of  $T_m$  for different cryoprotectant solutions: (a)  $X_W = 0.4$  and (b)  $X_W = 0.95$ . ● Experimental data.

frozen bovine plasma protein. However, it is also clearly shown that glucose significantly contributes to the depression of the freezing point in aqueous cryoprotectant solutions and that it can be used as an alternative to reduce or avoid intra- or extra-cellular ice formation during chilling and freezing processes [3, 4]. As previously discussed, intermediate values of  $T_g$ ,  $T_m'$ , and  $T_m$  were obtained for the other mixtures of cryoprotectants, resulting from the good compatibility and mutual plasticizing action of the different components in the samples [56, 57].

Although numerous studies have been conducted on the use of cryoprotectants to prevent deleterious changes in foods caused during freezing and frozen storage, little research has been carried out on the thermal transition properties of aqueous cryoprotectant solutions at frozen temperatures at a large working range of water contents. In this context, the experimental values of  $T_g'$ ,  $T_m'$ , and  $T_m$  (Table 1) obtained

and the mathematical models proposed in this study (Table 2) may be a great aid for the formulation of cryoprotective media containing more than two cryoprotectants to improve the storage stability and quality of frozen food products with high and intermediate moisture content and modifiable formulations, such as ice cream, purees, jams, surimi, sugared yolks, etc. However, further studies are required, which will focus on overcoming the difficulties in the incorporation of cryoprotectants in large samples or foodstuffs, such as whole fruits and meats.

#### 4. Conclusions

The effects of cryoprotectants and their concentration on the glass and phase transition temperatures of frozen aqueous solutions containing maltodextrin, polydextrose, glucose, and their mixtures prepared at moisture contents in the range

of 40–95% water were studied. DSC thermograms revealed the existence of a glass transition for pure maltodextrin solutions and two transitions for all the other solutions. The results indicated that the  $T_g'$ ,  $T_m'$ , and  $T_m$  values increase with the molecular weight of the cryoprotectant. Additionally, statistical analysis of the data ( $p < 0.05$ ) demonstrated that both the solute and water composition should be considered in the formulation of cryoprotective media, as they were found to significantly affect the  $T_g'$ ,  $T_m'$ , and  $T_m$  values ( $p < 0.05$ ). Mathematical expressions for  $T_g'$ ,  $T_m'$ , and  $T_m$  as a function of the mass fractions of the cryoprotectants ( $X_M$ ,  $X_G$ ,  $X_P$ ) and water ( $X_W$ ) and their interactions were developed to guide the formulation of cryoprotective media involving mixtures of more than two cryoprotectants to improve the storage stability and quality of frozen food products at high and intermediate moisture contents with modifiable formulations, such as ice cream, purees, jams, surimi, sugared yolks, etc.

### Data Availability

Data used to support the findings of this study are available from the corresponding author upon request.

### Conflicts of Interest

The authors declare no conflicts of interest.

### Acknowledgments

The authors wish to acknowledge the financial support from the Consejo Nacional de Ciencia y Tecnología for the Project FSSEP02-C-2017-18/A1-S-32348 and from the Fondo de Apoyo a la Investigación for the Project C18-FAI-05-64.64.

### References

- [1] P. Nesvadba, *Frozen Food Science and Technology*, J. A. Evans, Ed., chapter 1, Blackwell Publishing, Singapore, 2008.
- [2] C. Marella and K. Muthukumarappan, *Handbook of Farm, Dairy and Food Machinery Engineering*, M. Kutz, Ed., chapter 13, Academic Press, USA, 2013.
- [3] Z. Berk, *Food Process Engineering and Technology*, S. L. Taylor, Ed., chapter 19, Academic Press, USA, 2009.
- [4] S. J. James and C. James, "Food safety management," in *A Practical Guide for The Food Industry*, Y. Motarjemi, Ed., chapter 20, Academic Press, Bilthoven, The Netherlands, 2014.
- [5] L. D. Kaale, T. M. Eikevik, T. Rustad, and K. Kolsaker, "Super-chilling of food: A review," *Journal of Food Engineering*, vol. 107, no. 2, pp. 141–146, 2011.
- [6] G. G. Stonehouse and Z. Evans, "The use of supercooling for fresh foods: A review," *Journal of Food Engineering*, vol. 141, pp. 74–79, 2015.
- [7] Q. T. Pham and R. F. Mawson, *Quality in Frozen Food*, M. C. Erickson and Y. C. Hung, Eds., chapter 5, Springer-Science+Business Media, B.V., USA, 1997.
- [8] Q. T. Pham, "Advances in food freezing/thawing/freezing concentration modelling and techniques," *Japan Journal of Food Engineering*, vol. 9, no. 1, pp. 21–32, 2008.
- [9] B. De Ancos, C. Sánchez-Moreno, S. De Pascual-Teresa, and M. P. Cano, *Handbook of Fruits And Fruit Processing*, N. K. Sinha, J. S. Sidhu, J. Barta, J. S. B. Wu, and M. P. Cano, Eds., chapter 7, John Wiley & Sons, Ltd, USA, 2012.
- [10] R. G. M. Van Der Sman, A. Voda, G. Van Dalen, and A. Duijster, "Ice crystal interspacing in frozen foods," *Journal of Food Engineering*, vol. 116, no. 2, pp. 622–626, 2013.
- [11] A. J. Joshi, "A review and application of cryoprotectant: The science of cryonics," *PharmaTutor*, vol. 4, no. 1, pp. 12–18, 2016.
- [12] S. Charoenrein and N. Harnkarnsujarit, *Non-Equilibrium States And Glass Transitions in Foods. Processing Effects And Product-Specific Implications*, B. Bhandari and Y. Roos, Eds., chapter 2, Woodhead Publishing, UK, 2017.
- [13] H. D. Goff, "The use of thermal analysis in the development of a better understanding of frozen food stability," *Pure and Applied Chemistry*, vol. 67, no. 11, pp. 1801–1995, 1995.
- [14] M. Le Meste, D. Champion, G. Roudaut, G. Blond, and D. Simatos, "Glass transition and food technology: A critical appraisal," *Journal of Food Science*, vol. 67, no. 7, pp. 2444–2458, 2002.
- [15] S. Jittinandana, P. B. Kenney, and S. D. Slider, "Cryoprotectants affect physical properties of restructured trout during frozen storage," *Journal of Food Science*, vol. 70, p. C35, 2005.
- [16] P. Kittiphattanabawon, S. Benjakul, W. Visessanguan, and F. Shahidi, "Cryoprotective effect of gelatin hydrolysate from blacktip shark skin on surimi subjected to different freeze-thaw cycles," *LWT- Food Science and Technology*, vol. 47, no. 2, pp. 437–442, 2012.
- [17] R. M. Syamaladevi, K. N. Manahiloh, B. Muhunthan, and S. S. Sablani, "Understanding the influence of state/phase transitions on ice recrystallization in atlantic salmon (*salmo salar*) during frozen storage," *Food Biophysics*, vol. 7, no. 1, pp. 57–71, 2012.
- [18] N. E. Zaritzky, *Frozen Food Science And Technology*, J. A. Evans, Ed., chapter 11, Blackwell Publishing, Singapore, 2008.
- [19] Y. H. Roos, "Glass Transition Temperature and Its Relevance in Food Processing," *Annual Review of Food Science and Technology*, vol. 1, pp. 469–496, 2010.
- [20] S. S. Sablani, R. M. Syamaladevi, and B. G. Swanson, "A review of methods, data and applications of state diagrams of food systems," *Food Engineering Reviews*, vol. 2, no. 3, pp. 168–203, 2010.
- [21] A. Pyne, R. Surana, and R. Suryanarayanan, "Enthalpic relaxation in frozen aqueous trehalose solutions," *Thermochimica Acta*, vol. 405, no. 2, pp. 225–234, 2003.
- [22] C. L. M. Silva, E. M. Goncalves, and T. R. S. Brandao, *Frozen Food Science And Technology*, J. A. Evans, Ed., chapter 8, Blackwell Publishing, Singapore, 2018, Blackwell Publishing.
- [23] R. M. Syamaladevi, S. S. Sablani, J. Tang, J. Powers, and B. G. Swanson, "Stability of anthocyanins in frozen and freeze-dried raspberries during long-term storage: in relation to glass transition," *Journal of Food Science*, vol. 76, no. 6, pp. E414–E421, 2011.
- [24] A. Grajales-Lagunes, A. J. Flores-Ramírez, R. González-García et al., "The role of the glass transition temperature of the maximally-freeze-concentrated phase in the storage stability of frozen escamoles (*Liometopum apiculatum* M.)," *Revista Mexicana de Ingeniería Química*, vol. 17, no. 2, pp. 739–752, 2018.
- [25] M. Karel and I. Saguy, *Water Relationships in Food*, H. Levine and L. Slade, Eds., chapter 7, Plenum Press, New York, NY, USA, 1991.



- [26] M. S. Rahman, "State diagram of date flesh using differential scanning calorimetry (DSC)," *International Journal of Food Properties*, vol. 7, no. 3, pp. 407–428, 2004.
- [27] Y. Yu and H. Li, "State diagrams of freeze dried colostral whey powders: Effects of additives on the stability of colostral whey powders," *Journal of Food Science*, vol. 10, pp. 117–126, 2012.
- [28] C. Vásquez, P. Díaz-Calderón, J. Enrione, and S. Matiacevich, "State diagram, sorption isotherm and color of blueberries as a function of water content," *Thermochimica Acta*, vol. 570, pp. 8–15, 2013.
- [29] L. A. Schaller-Povolny, D. E. Smith, and T. P. Labuza, "Effect of water content and molecular weight on the moisture isotherms and glass transition properties of inulin," *Journal of Food Science*, vol. 3, no. 2, pp. 173–192, 2000.
- [30] Y. Roos and M. Karel, "Water and molecular weight effects on glass transitions in amorphous carbohydrates and carbohydrate solutions," *Journal of Food Science*, vol. 56, no. 6, pp. 1676–1681, 1991.
- [31] Y. Roos and M. Karel, "Phase transitions of mixtures of amorphous polysaccharides and sugars," *Biotechnology Progress*, vol. 7, no. 1, pp. 49–53, 1991.
- [32] C. Ohkuma, K. Kawai, C. Viriyarattanasak et al., "Glass transition properties of frozen and freeze-dried surimi products: Effects of sugar and moisture on the glass transition temperature," *Food Hydrocolloids*, vol. 22, no. 2, pp. 255–262, 2008.
- [33] M. A. Ruiz-Cabrera, C. Rivera-Bautista, A. Grajales-Lagunes, R. González-García, and S. J. Schmidt, "State diagrams for mixtures of low molecular weight carbohydrates," *Journal of Food Engineering*, vol. 171, pp. 185–193, 2016.
- [34] P. A. Carvajal, G. A. MacDonald, and T. C. Lanier, "Cryostabilization mechanism of fish muscle proteins by maltodextrins," *Cryobiology*, vol. 38, no. 1, pp. 16–26, 1999.
- [35] T. Maity, A. Saxena, and P. S. Raju, "Use of hydrocolloids as cryoprotectant for frozen foods," *Critical Reviews in Food Science and Nutrition*, vol. 58, no. 3, pp. 420–435, 2018.
- [36] M. A. Da Silva, P. J. A. Sobral, and T. G. Kieckbusch, "Phase transitions of frozen camu-camu (*Myrciaria dubia* (HBK) McVaugh) pulp: Effect of cryostabilizer addition," *Food Biophysics*, vol. 3, no. 3, pp. 312–317, 2008.
- [37] G. A. MacDonald and T. C. Lanier, *Quality in Frozen Foods*, M. C. Erickson and Y. C. Hung, Eds., chapter 11, Springer-Science+Business Media, B.V., USA, 1997.
- [38] A. Santove, M. J. Piñero, and M. Llabrés, "Comparison between DSC and TMDSC in the investigation into frozen aqueous cryoprotectants solutions," *Drug Development and Industrial Pharmacy*, vol. 36, no. 12, pp. 1413–1421, 2010.
- [39] N. Harnkarnsujarit, M. Nakajima, K. Kawai, M. Watanabe, and T. Suzuki, "Thermal properties of freeze-concentrated sugar-phosphate solutions," *Food Biophysics*, vol. 9, pp. 213–218, 2014.
- [40] J. R. Herrera and I. M. Herrera, "Cryoprotection of frozen-stored actomyosin of farmed rainbow trout (*Oncorhynchus mykiss*) by some sugars and polyols," *Food Chemistry*, vol. 84, pp. 97–104, 2004.
- [41] M. Dziomdziora, L. Krala, and J. Food Nutr, "Cryoprotection of pork," *International Journal of Food Sciences and Nutrition*, vol. 15/56, no. 1, pp. 23–26, 2006.
- [42] D. Kovačević, K. Mastanjević, and J. Kordić, "Cryoprotective effect of polydextrose on chicken surimi," *Czech Journal of Food Sciences*, vol. 29, no. 3, pp. 226–231, 2011.
- [43] L. T. Rodríguez Furlán, J. Lecot, A. Pérez Padilla, M. E. Campderrós, and N. Zaritzky, "Effect of saccharides on glass transition temperatures of frozen and freeze dried bovine plasma protein," *Journal of Food Engineering*, vol. 106, no. 1, pp. 74–79, 2011.
- [44] J. J. Rodríguez-Herrera, M. Bernárdez, G. Sampedro, M. L. Cabo, L. Pastoriza, and J. Agric, "Possible role for cryostabilizers in preventing protein and lipid alterations in frozen-stored minced muscle of Atlantic mackerel," *Journal of Agricultural and Food Chemistry*, vol. 54, no. 9, pp. 3324–3333, 2006.
- [45] P. A. Carvajal, G. A. McDonald, and T. C. Lanier, "Cryostabilization mechanism of fish muscle proteins by maltodextrins," *Cryobiology*, vol. 38, no. 1, pp. 16–26, 1999.
- [46] J. J. Rodríguez-Herrera, L. Pastoriza, and G. Sampedro, "Effects of various cryostabilisers on protein functionality in frozen-stored minced blue whiting muscle: The importance of inhibiting formaldehyde production," *European Food Research and Technology*, vol. 214, no. 5, pp. 382–387, 2002.
- [47] N. Harnkarnsujarita, S. Charoenreina, and Y. H. Roos, "Microstructure formation of maltodextrin and sugar matrices in freeze-dried systems," *Carbohydrate Polymers*, vol. 88, no. 2, pp. 734–742, 2012.
- [48] Official Methods of Analysis, *Association of Official Analytical Chemists*, Washington, USA, 15th edition edition, 1996.
- [49] J. H. Zhao, F. Liu, X. Wen, H. W. Xiao, and Y. Y. Ni, "State diagram for freeze-dried mango: freezing curve, glass transition line and maximal-freeze-concentration condition," *Journal of Food Engineering*, vol. 157, pp. 49–56, 2015.
- [50] S. Ablett, M. J. Izzard, and P. J. Lillford, "Differential scanning calorimetric study of frozen sucrose and glycerol solutions," *Journal of the Chemical Society, Faraday Transactions*, vol. 88, no. 6, p. 789, 1992.
- [51] H. Goff, E. Verespej, and D. Jermann, "Glass transitions in frozen sucrose solutions are influenced by solute inclusions within ice crystals," *Thermochimica Acta*, vol. 399, no. 1–2, pp. 43–55, 2003.
- [52] H. Goff and M. Sahagian, "Glass transitions in aqueous carbohydrate solutions and their relevance to frozen food stability," *Thermochimica Acta*, vol. 280–281, pp. 449–464, 1996.
- [53] K. S. Pehkonen, Y. H. Roos, S. Miao, R. P. Ross, and C. J. Stanton, "State transitions and physicochemical aspects of cryoprotection and stabilization in freeze-drying of *Lactobacillus rhamnosus* GG (LGG)," *Journal of Applied Microbiology*, vol. 104, no. 6, pp. 1732–1743, 2008.
- [54] G. A. Sacha and S. L. Nail, "Thermal analysis of frozen solutions: multiple glass transitions in amorphous systems," *Journal of Pharmaceutical Sciences*, vol. 98, no. 9, pp. 3397–3405, 2009.
- [55] N. Harnkarnsujarit, S. Charoenrein, and Y. H. Roos, "Microstructure formation of maltodextrin and sugar matrices in freeze-dried systems," *Carbohydrate Polymers*, vol. 88, no. 2, pp. 734–742, 2012.
- [56] V. B. Tolstoguzov, "The importance of glassy biopolymer components in food," *Nahrung-Food*, vol. 44, no. 2, pp. 76–84, 2000.
- [57] K. J. Singh and Y. H. Roos, "Frozen state transitions of sucrose/protein/cornstarch mixtures," *Journal of Food science*, vol. 70, no. 3, pp. E198–E204, 2005.
- [58] Y. J. Wang and J. Jane, "Correlation between glass transition temperature and starch retrogradation in the presence of sugars and maltodextrins," *Cereal Chemistry*, vol. 71, no. 6, pp. 527–531, 1994.

## RESUMEN EN EXTENSO 2

### The Influence of Maltodextrin on the Thermal Transitions and State Diagrams of Fruit Juice Model Systems

#### INTRODUCCIÓN

Un diagrama de estado es una representación gráfica de los distintos estados físicos y transiciones de fase/estado que ocurren en un material en función del contenido de sólidos y la temperatura (Rahman, 2010). El diagrama de estado generalmente, incluye la curva de congelación en función del contenido de sólidos ( $T_m$  vs  $X_s$ ), la curva de transición vítrea en función del contenido de sólidos ( $T_g$  vs  $X_s$ ) y la condición de máxima crio-concentración. Estos diagramas han sido de gran ayuda para monitorear el progreso y desarrollo de varias operaciones unitarias como la congelación, el almacenamiento en congelado, liofilización, crio-concentración, deshidratación y secado por aspersion, que se utilizan para extender la vida útil de los alimentos y generar una gama de productos de frutas de humedad alta, intermedia y baja. En este contexto, la curva del punto de congelación ( $T_m$  vs  $X_s$ ) y las temperaturas de transición de fase máximamente crioconcentrada  $T_g'$  y  $T_m'$  pueden ser utilizadas para prevenir cambios físicos, químicos y estructurales que tienen lugar durante el almacenamiento en congelado de frutas frescas, y para evitar la reducción de volumen o colapso del alimento que se presenta durante la liofilización de materiales biológicos (Celli et al., 2016). Las temperaturas  $T_g'$  y  $T_m'$  son consideradas como parámetros de referencia para determinar la estabilidad de los alimentos congelados, porque se produce la máxima formación de hielo cuando los sistemas alimentarios se almacenan a estas temperaturas. Por otro lado, la relación  $T_g$  y  $X_s$  se ha considerado en la literatura como parámetro de referencia para determinar las condiciones adecuadas de proceso de secado y la estabilidad de almacenamiento de productos de baja humedad (Bhandari & Howes. 1999). En estos casos, las transformaciones estructurales dependientes tiempo, como la adherencia y deposición que ocurren en el sacado por aspersion o el apelmazamiento y los

fenómenos de cristalización que tienen lugar durante el almacenamiento de frutas en polvo, depende en gran medida del valor  $T_g$ . En la literatura se ha encontrado que los valores  $T_g'$ ,  $T_m'$  y  $T_g$  de los productos de fruta son muy bajo del orden de  $-71$  a  $-38^\circ\text{C}$ ,  $-52$  a  $-26^\circ\text{C}$ , y de  $12$  a  $75^\circ\text{C}$ , respectivamente. Se ha recomendado el uso de polímeros como crioprotectores durante el almacenamiento en congelado y como agente acarreador en los procesos de secado para manipular el estado físico y elevar deliberadamente los valores de  $T_g'$ ,  $T_m'$  y la  $T_g$  de los alimentos (Flores-Ramírez et al., 2019). El uso de carbohidratos de alto peso molecular en la construcción de diagramas de estado para productos de frutas no se ha explorado ampliamente. Solo han sido algunos estudios que han informado de diagramas de algunas frutas con maltodextrina. Ya que los componentes sólidos de las frutas son glucosa, fructosa, sacarosa, ácido cítrico y pectina se planteó hacer sistemas modelos basados en las diversas composiciones de las diferentes variedades de frutas (Fabra et al., 2009). Esto con la finalidad de controlar la composición de cada sistema y evaluar el efecto de la maltodextrina sobre los valores de  $T_g'$ ,  $T_m'$  y la  $T_g$ .

## **OBJETIVOS**

1. Evaluar el efecto de la maltodextrina en los valores de  $T_g'$ ,  $T_m'$ ,  $T_m$  y  $T_g$  de diferentes sistemas de modelos de jugos de frutas preparados con diversos contenidos de agua mediante el uso de calorimetría diferencial de barrido (DSC),
2. Construir los diagramas de estados de diferentes sistemas modelo de jugos de frutas.
3. Evaluar la influencia de la composición química en las transiciones térmicas  $T_g'$ ,  $T_m'$ ,  $T_m$  y  $T_g$ .

## **MATERIALES Y MÉTODOS**

Glucosa, fructosa, sacarosa, pectina y ácido cítrico fueron utilizados para formular sistemas modelo de jugos de frutas adicionados con fracciones máxicas de maltodextrina de 0 a 0.8. Un diseño D-Optimal para mezclas de 6 componentes fue

utilizado con las siguientes restricciones:  $0 \leq X_M \leq 0.8$ ;  $0 \leq X_P \leq 0.15$ ;  $0 \leq X_A \leq 0.15$ ;  $X_G + X_S + X_F + X_A + X_P + X_M = 1$ . Un total de 25 sistemas anhidros fueron obtenidos. Para la obtención de los diferentes diagramas de estado fue necesario un acondicionamiento de los sistemas modelo anhidros. Para humedades menores a 50% se realizó mediante exposición directa a humedad relativa del 100 %. Para muestras con humedades superiores a 50% se realizó el acondicionamiento mediante la adición directa de agua. Muestras de 10 mg fueron tomadas de cada sistema modelo acondicionado y colocadas en charolas DSC (TA Instruments), las cuales fueron selladas herméticamente y se dejaron en equilibrio durante 24 horas. Todos los análisis térmicos fueron realizados en un Calorímetro Diferencial de Barrido (DSC Q2000 (TA Instruments)). Las muestras fueron sometidas a un método de escaneo convencional lineal el cual consistió en un enfriamiento a  $-90^\circ\text{C}$  a una velocidad de  $20^\circ\text{C}/\text{min}$ , esta temperatura se mantuvo durante 5 min, y posteriormente fueron calentadas hasta  $20^\circ\text{C}$  a  $10^\circ\text{C}/\text{min}$ . Para muestras con una humedad de 20-50 % (b.h.) fue requerido un procedimiento de annealing a  $T_m' - 1^\circ\text{C}$  con el fin de maximizar la formación de hielo. Mientras que para muestras con XM predominante, fue necesario someter las muestras a un calentamiento desde la temperatura ambiente hasta  $80^\circ\text{C}$  a  $20^\circ\text{C}/\text{min}$ . Para muestras anhidras o muestras con agua no congelable el protocolo de melt-quenching fue utilizado. Los valores de  $T_g'$  y  $T_m'$  fueron respectivamente asignados al punto medio del 1° y 2° paso de cambio de flujo de calor observados en los termogramas durante el calentamiento. La temperatura máxima correspondiente a la endoterma de fusión fue considerada como el punto de congelación ( $T_m$ ). Posteriormente se realizaron los diagramas de estado para cada sistema modelo y se obtuvieron los modelos de las curvas  $T_m$  y  $T_g$  con la ecuaciones de Chen y Gordon- Taylor, respectivamente.

## RESULTADOS

En los diferentes sistemas modelo de jugos de frutas preparados en rangos de agua congelable entre 30 al 90% en base húmeda, mostraron tres eventos térmicos en los que el pico endotérmico de fusión del hielo fue el rango más visible, así mismo

se visualizaron dos cambios en la línea base característicos de transición de estado. Para soluciones de azúcar se ha sugerido que la primera transición de estado se atribuye a la transición vítrea de la fase máximamente crioconcentrada ( $T_g'$ ) y la segunda transición considerarse como el comienzo del derretimiento de los cristales de hielo ( $T_m'$ ). La primera transición se observó en los diferentes sistemas modelos en rangos de  $-9.5$  a  $-57.1^\circ\text{C}$ , y la segunda transición entre  $-9.5$  a  $-42.8^\circ\text{C}$ . Los valores más altos fueron obtenidos en sistemas modelo con fracciones másicas de maltodextrina superiores o iguales a  $0.4$ . Con lo que respecta a los sistemas modelo acondicionados a humedades reducidas de  $0$  a  $29\%$  base húmeda, se pudo observar que las muestras presentaron un desplazamiento endotérmico debido a la transición vítrea con valores de  $157$  a  $-0.3^\circ\text{C}$ . Cuanto mayor fue la concentración de sólidos, los valores de  $T_g$  de los sistemas modelo fueron más elevados. La transición vítrea se produjo en un amplio rango de temperatura (alrededor de  $40$ - $50^\circ\text{C}$ ), esto debido a la presencia de maltodextrina. Los diagramas de estado obtenidos fueron afectados significativamente ( $p < 0.05$ ) por la composición química de los sistemas modelo, además se observó un aumento en el valor de los parámetros  $t_g'$ ,  $t_m'$  y  $t_g$  con lo cual los valores de estos parámetros están más cercanos a los rangos de temperatura utilizados en los procesos de congelación y deshidratación. Así mismo, se obtuvieron modelos matemáticos que permiten estimar el valor de los parámetros de los diagramas de estado en función de la composición de sólidos de las frutas, por lo que es posible construir diagramas de estado y predecir los efectos que tendrá la adición de maltodextrina sobre una amplia gama de productos derivados de las frutas.

## **CONCLUSIÓN**

Se investigaron los efectos de la adición de maltodextrina sobre  $T_g'$ ,  $T_m'$ ,  $T_m$  y  $T_g$  durante la construcción de diagramas de estado de varios sistemas de modelos de jugo de frutas. El aumento de la fracción másica de maltodextrina dio como resultado un aumento significativo de las transiciones térmicas antes mencionadas. Sin embargo, se requieren fracciones de masa superiores a  $0,4$  para inducir un aumento

significativo de  $T_g'$ ,  $T_m'$ ,  $T_m$  y la curva  $T_g$ . La maltodextrina, por tanto, puede considerarse como una buena alternativa en la formulación de medios crioprotectores para una adecuada conservación congelada de alimentos de humedad alta e intermedia, y como agente portador en el proceso de secado por atomización. Los modelos matemáticos desarrollados facilitaron la determinación de la influencia de la composición química sobre los valores  $T_{gs}$ ,  $K$ ,  $E$ ,  $B$ ,  $T_m$ ,  $T_g'$ ,  $T_m'$  y  $x_s'$ , y también podría utilizarse para predecir los diagramas de estado de muestras en función de la concentración de solutos predominantes en jugos de frutas y la fracción másica de maltodextrina, ayudando en el diseño y optimización de procesos y procedimientos de almacenamiento de productos frutales en rangos de humedad alta, intermedia y baja.

## **BIBLIOGRAFÍA**

1. Bhandari, B. R. & Howes, T. (1999). Implication of glass transition for the drying and stability of dried foods. *J. Food Eng.* 40, 71–79.
2. Celli, G. B., Ghanem, A. & Brooks, M. S. L. (2016). Influence of freezing process and frozen storage on the quality of fruits and fruit products. *Food Rev.* 32, 280–304.
3. Fabra, M. J., Talens, P., Moraga, G. & Martínez-Navarrete, N. (2009). Sorption isotherm and state diagram of grapefruit as a tool to improve product processing and stability. *J. Food Eng.* 93, 52–58.
4. Flores-Ramírez, A. J., García-Coronado, P., Grajales-Lagunes, A., González-García, R., Abud Archila, M. & Ruiz-Cabrera, M. A. (2019). Freeze-concentrated phase and state transition temperatures of mixtures of low and high molecular weight cryoprotectants. *Adv. Polym. Technol.* 5341242
5. Rahman, M. S. (2010). Food stability determination by macro-micro region concept in the state diagram and by defining a critical temperature. *J. Food Eng.* 99, 402–416.

# RESUMEN GRÁFICO 2

Sistemas modelo de jugos de frutas



Acondicionamiento de humedad



Humedad baja 1–29 %  
Humedad intermedia 30–50%



Humedad alta 60 – 90 %

Análisis calorimétrico



Caracterización térmica de sistemas modelo

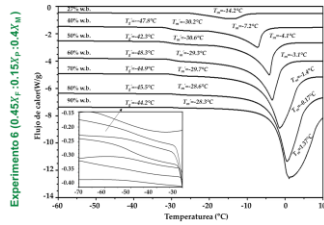
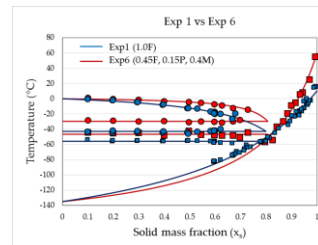


Diagrama de estado



Article

# The Influence of Maltodextrin on the Thermal Transitions and State Diagrams of Fruit Juice Model Systems

Pedro García-Coronado <sup>1</sup>, Alma Flores-Ramírez <sup>1</sup>, Alicia Grajales-Lagunes <sup>1</sup>, Cesar Godínez-Hernández <sup>2</sup>, Miguel Abud-Archila <sup>3</sup>, Raúl González-García <sup>1</sup> and Miguel A. Ruiz-Cabrera <sup>1,\*</sup>

<sup>1</sup> Faculty of Chemical Sciences, Autonomous University of San Luis Potosí, Manuel Nava 6, 78290 San Luis Potosí, Mexico; pgarciam16@gmail.com (P.G.-C.); aalmaramirez@hotmail.com (A.F.-R.); grajales@uaslp.mx (A.G.-L.); raulgg@uaslp.mx (R.G.-G.)

<sup>2</sup> Desert Zones Research Institute, Autonomous University of San Luis Potosí, Altair 200, 78377 San Luis Potosí, Mexico; cesar.godinez@uaslp.mx

<sup>3</sup> National Institute of Technology of Mexico, Technological Institute of Tuxtla Gutiérrez, Street Km 1080, Tuxtla Gutiérrez 29050, Mexico; miaba69@hotmail.com

\* Correspondence: mruiz@uaslp.mx

Received: 27 August 2020; Accepted: 10 September 2020; Published: 12 September 2020



**Abstract:** The state diagram, which is defined as a stability map of different states and phases of a food as a function of the solid content and temperature, is regarded as fundamental approach in the design and optimization of processes or storage procedures of food in the low-, intermediate-, and high-moisture domains. Therefore, in this study, the effects of maltodextrin addition on the freezing points ( $T'_m$ ,  $T_m$ ) and glass transition temperatures ( $T'_g$ ,  $T_g$ ) required for the construction of state diagrams of fruit juice model systems by using differential scanning calorimetry methods was investigated. A D-optimal experimental design was used to prepare a total of 25 anhydrous model food systems at various dry mass fractions of fructose, glucose, sucrose, pectin, citric acid, and maltodextrin, in which this last component varied between 0 and 0.8. It was found that maltodextrin mass fractions higher than 0.4 are required to induce significant increases of  $T'_g$ ,  $T'_m$ ,  $T_g$ , and  $T_m$  curves. From this perspective, maltodextrin is a good alternative as a cryoprotectant and as a carrier agent in the food industry. Furthermore, solute-composition-based mathematical models were developed to evaluate the influence of the chemical composition on the thermal transitions and to predict the state diagrams of fruit juices at different maltodextrin mass fractions.

**Keywords:** state diagrams; maltodextrin; thermal transitions; DSC; model systems

## 1. Introduction

A state diagram is a graphical map of the different states of a food or biomaterial as a function of temperature over the entire solid mass fraction scale of materials containing freezable and unfreezable water [1–4]. In this context, a state diagram usually includes the freezing curve as a function of the solid content ( $T_m$  vs.  $w_s$ ), the glass transition curve as a function of the solid content ( $T_g$  vs.  $w_s$ ), and the maximal-freeze-concentration condition, defined by the onset melting temperature of ice crystals ( $T'_m$ ), the glass transition temperature at maximum ice formation conditions ( $T'_g$ ), and the solid mass fraction ( $w'_s$ ) [1–4]. These diagrams have been of great help in monitoring the progress and development of various employed unit operations, such as freezing, frozen storage, lyophilization, cryoconcentration, dehydration, and spray drying, which are all used to extend shelf life and to generate a range of high-, intermediate-, and low-moisture fruit products, such as whole fruits, cut fruits, juices, purees, jams,



marmalades, dried fruits, powders, and leathers [1,2,4–9]. For instance, the freezing curves ( $T_m$  vs.  $w_s$ ) and the freeze-concentrated unfrozen phase transition temperatures  $T'_g$  and  $T'_m$  of products can be used to prevent physical, chemical, and structural changes that take place during the frozen storage of fresh and cut fruits and to avoid the product shrinkage or collapse usually observed during the freeze drying of biological materials [5,10–14]. The temperatures  $T'_g$  and  $T'_m$  are regarded as reference parameters determining the stability of frozen foods, because maximum ice formation takes place when food systems are stored between these temperatures [2,15]. As a general statement, the formation of a glassy vitreous state is then required in frozen storage to prevent molecular motion and further crystallization of water into ice, as well as in freeze drying, because collapse during primary drying will occur when the product temperature exceeds the collapse temperature, which is normally a few degrees above the  $T'_g$  value [10–14]. On the other hand, the relationship between  $T_g$  and  $w_s$  in the solid mass fraction domain of  $w'_s \leq T_g \leq 1$  has also been regarded in the literature as a reference parameter determining the suitable conditions of drying processes and the storage stability of low-moisture food products. In these cases, the various time-dependent structural transformations, such as the stickiness and deposition events occurring on the dryer surface during spray drying or caking and the crystallization phenomena that take place during fruit powder storage, are highly dependent on  $T_g$  values [16,17].

For these purposes, several state diagrams of pure components, model food systems, and real fruit products have been reported in the literature [4,18–26]. Nevertheless, from the above studies it was found that fruit products presented very low  $T'_g$ ,  $T'_m$ , and anhydrous sample glass transition ( $T_{gs}$ ) values, which ranged from  $-71$  to  $-38$  °C, from  $-52$  to  $-26$  °C, and from  $12$  to  $75$  °C, respectively. Thus, it is sometimes not possible to design suitable, efficient, and economical processes and frozen storage procedures for sugar-rich products such as fruits [2,11]. The use of polymers as cryoprotectants during frozen storage and as carrier agents in spray drying processes to manipulate the physical state and deliberately elevate the  $T'_g$ ,  $T'_m$ , and  $T_g$  of foods has been widely recommended [11,27–32]. Typically, polymers with high molecular weight (HMW), such as maltodextrin, polydextrose, hydrocolloids, and gum, have been used [11,14,28–33]. The use of HMW carbohydrates in the construction of state diagrams for fruit products has not been explored extensively, and there are only a few studies in which the state diagrams of some fruits with a maltodextrin addition have been reported [34–36]. On the other hand, water and soluble solids such as sugars, pectin, and organic acids are the main fruit components, and the amount of each of these constituents can change drastically from one fruit to another. Furthermore, the number of possible fruit compositions is great. Therefore, experiments with fruit juice model systems with controlled chemical compositions are required. The aim of the present work is (i) to evaluate the effect of maltodextrin on the  $T'_g$ ,  $T'_m$ ,  $T_m$ , and  $T_g$  values of different fruit juice model systems prepared with various water contents by using differential scanning calorimetry (DSC), (ii) to construct the corresponding state diagrams, and (iii) to evaluate the influence of the chemical composition on the abovementioned thermal transitions.

## 2. Materials and Methods

### 2.1. Materials

Analytical-grade maltodextrin dextrose equivalent 4–7 (product No. 419672; molecular weight (MW) 3600, Sigma-Aldrich Co. St. Louis, MO, USA), crystalline fructose (product No. F2543; MW 180.16, Sigma-Aldrich Co. St. Louis, MO, USA), glucose (product No. G7528; MW 180.2, Sigma-Aldrich Co. St. Louis, MO, USA), sucrose (product No. S0389; MW 342.3, Sigma-Aldrich Co. St. Louis, MO, USA), citric acid (product No. 251275; MW 192.12, Sigma-Aldrich Co. St. Louis, MO, USA), and pectin from apples (product No. 76282, MW 208.2, Sigma-Aldrich Co. St. Louis, MO, USA) were purchased and used without further treatment in the experiments.

### 2.2. Preparation of Fruit Juice Model Systems

A completely randomized D-optimal experimental design for mixtures of six components was used to prepare a total of 25 anhydrous model food systems at various dry mass fractions of fructose ( $X_F$ ), glucose ( $X_G$ ), sucrose ( $X_S$ ), citric acid ( $X_A$ ), pectin ( $X_P$ ), and maltodextrin ( $X_M$ ), as shown in Table 1. The studies carried out by Grajales-Lagunes et al. [4] and Fongin et al. [37,38] were considered as references to establish the mass fractions of citric acid ( $0 \leq X_A \leq 0.15$ ), pectin ( $0 \leq X_P \leq 0.15$ ), and maltodextrin ( $0 \leq X_M \leq 0.8$ ) in the model food systems.

**Table 1.** D-optimal experimental design for a mixture of six components and the elaboration of anhydrous model food systems.

Experiment		Mass Fractions					
no.	Ro	$X_F$	$X_G$	$X_S$	$X_P$	$X_A$	$X_M$
1	15	1	0	0	0	0	0
2	6	0	1	0	0	0	0
3	8	0	0	1	0	0	0
4	4	0	0	0	0.15	0.05	0.80
5	1	0.283	0.283	0.283	0.075	0.075	0
6	7	0.45	0	0	0.15	0	0.40
7	21	0	0.45	0	0.15	0	0.40
8	2	0	0	0.45	0.15	0	0.40
9	23	0.50	0	0.50	0	0	0
10	22	0	0.50	0.50	0	0	0
11	18	0.50	0.50	0	0	0	0
12	24	0.145	0.145	0.145	0.059	0.15	0.355
13	20	0.70	0	0	0.15	0.15	0
14	5	0	0.70	0	0.15	0.15	0
15	11	0	0	0.70	0.15	0.15	0
16	25	0.327	0.327	0.077	0.035	0.035	0.198
17	19	0.327	0.077	0.327	0.035	0.035	0.198
18	12	0.077	0.327	0.327	0.035	0.035	0.198
19	3	0.177	0.077	0.077	0.035	0.035	0.598
20	9	0.502	0.077	0.077	0.035	0.110	0.198
21	13	0.077	0.540	0.077	0.035	0.073	0.198
22	14	0.077	0.077	0.577	0.035	0.035	0.198
23	10	0.35	0.35	0	0.15	0.15	0
24	17	0.35	0	0.35	0.15	0.15	0
25	16	0	0.35	0.35	0.15	0.15	0

no = number, Ro = Run order.

In order to obtain uniform mixing for the component mixtures, the procedure of complete dissolution followed by freeze drying was used for each of the model systems. Thus, solutions with 60% water were prepared, then frozen at  $-60\text{ }^\circ\text{C}$  using a laboratory freezer (ScientTemp Model 86-01A Adrian, Michigan, USA) for 24 h and dried at  $-40\text{ }^\circ\text{C}$  with a 5-mTorr vacuum using a freeze dryer (IlshinBioBase, TFD8501, Seoul, Korea). After complete drying, the freeze-dried mixtures were transferred to a pestle and mortar where they were ground into a fine powder. These samples were then equilibrated over Drierite<sup>®</sup> (anhydrous calcium sulfate,  $aw \approx 0$ ) in desiccators at room temperature for at least 4 weeks to obtain completely dried samples. Afterwards, these equilibrated freeze-dried mixtures were conditioned in the low, intermediate, and high moisture domains following the methodologies proposed by Grajales-Lagunes et al. [4] and Ruiz-Cabrera et al. [22], then subjected to the calorimetric analysis described below, in which the freezing points ( $T'_m, T_m$ ) and glass transition temperatures ( $T'_g, T_g$ ) for various water contents were determined.

### 2.3. Determination and Modeling of the Thermal Transition by DSC

A Q2000 differential scanning calorimeter (TA Instruments, New Castle, Delaware, USA) equipped with an RCS90 cooling system and Universal Analysis 2000<sup>®</sup> software for data treatment were used. The measurements were carried out in an inert atmosphere using nitrogen at a flow rate of 50 mL/min. An empty DSC pan as a reference and samples of about 10 mg were used in all of the cases. The standard mode with the linear temperature program was used to determine the freezing points and glass transition temperatures in samples containing freezable water [4,26]. Samples contained in sealed pans were cooled at 20 °C/min from room temperature to −90 °C, equilibrated for 5 min, and then heated to 20 °C at a heating rate of 10 °C/min. For the samples in the concentration range of 20% and 50% water, the previous calorimetry protocol was used with annealing at the apparent value of the freezing point ( $T'_m - 1$  °C) as the additional treatment to maximize ice formation in the samples [4,26]. In these cases, the samples were then equalized in the DSC at 20 °C, cooled to −90 °C at 20 °C/min, held for 2 min, warmed at 20 °C/min to the annealing temperature ( $T'_m - 1$  °C), kept for 30 min, recooled to −90 °C at 20 °C/min, held for 5 min, and finally scanned to 20 °C at 10 °C/min. The  $T'_g$  and  $T'_m$  values were assigned to the midpoint of the first and second step changes, respectively, of the observed heat flow and temperature relationship during the heating process, whereas the freezing point ( $T_m$ ) was determined from the peak temperature in the melting endotherm [4,22,26]. For anhydrous solids and samples containing unfreezable water, the calorimeter melt-quenching protocol was used [4,22]. The samples contained in sealed pans were first equilibrated in the DSC at 20 °C, then heated at 20 °C/min to the corresponding melting temperature using a holding time of 2 min. Afterwards, the samples were cooled to −90 °C at 20 °C/min and maintained there for 2 min. Finally, the samples were reheated at 10 °C/min again to the corresponding melting temperature. The midpoint  $T_g$  value was determined using the half-height method from the reheating DSC thermograms.

In order to construct state diagrams for each model system, the Gordon–Taylor (G-T) equation (Equation (1)) and Chen equation (Equation (2)) were used to model the glass transition curve ( $T_g$  vs.  $w_s$ ) and freezing point curve ( $T_m$  vs.  $w_s$ ), respectively, as follows [2,21,26]:

$$T_{gm} = \frac{w_s T_{gs} + K(1 - w_s) T_{gw}}{w_s + K(1 - w_s)} \quad (1)$$

$$T_m = T_w + \left( \frac{\beta}{\lambda_w} \right) \ln \left( \frac{1 - w_s - Bw_s}{1 - w_s - Bw_s + Ew_s} \right) \quad (2)$$

In Equation (1),  $T_{gm}$ ,  $T_{gs}$ , and  $T_{gw}$  are the glass transition temperatures of the sample, anhydrous solids, and amorphous water (−135 °C), respectively. In addition,  $w_s$  is the mass fraction of solids and  $K$  is a constant parameter denoting the strength of the interaction between the water and the food solids [1,2]. In Equation (2),  $T_m$  and  $T_w$  are the freezing temperatures of the sample and pure water, respectively;  $\beta$  is the molar freezing point constant of water (1860 kg K/kgmol) [2,21,26]. Moreover,  $\lambda_w$  and  $\lambda_s$  are the molecular mass values of water and solids, respectively;  $E$  is the molecular mass ratio of water-to-solids ( $\frac{\lambda_w}{\lambda_s}$ ). Finally,  $B$  is the ratio of unfreezable water from the total solid content. A nonlinear regression analysis by the least squares method was performed to estimate the parameters  $T_{gs}$ ,  $K$ ,  $E$ , and  $B$  by using Microsoft Excel (2016). The goodness of the fitted models was determined by the coefficient of determination ( $R^2$ ).

On the other hand, the procedure proposed by Grajales-Lagunes et al. [4] and Zhao et al. [26] was used to estimate the corresponding average values of  $T'_g$  and  $T'_m$ , as well as the values of  $w'_s$  from each of the constructed state diagrams.

## 2.4. Statistical Analysis

A polynomial equation (Equation (3)) was used to evaluate the effects of the weight fractions of fructose ( $X_F$ ), glucose ( $X_G$ ), sucrose ( $X_S$ ), citric acid ( $X_A$ ), pectin ( $X_P$ ) and maltodextrin ( $X_M$ ) on the parameters  $T_{gs}$ ,  $K$ ,  $E$ ,  $B$ ,  $T'_g$ ,  $T'_m$ , and  $w'_s$ , as follows:

$$y = a_1X_F + a_2X_G + a_3X_S + a_4X_P + a_5X_A + a_6X_M + a_7X_FX_G + a_8X_FX_S + a_9X_FX_P + a_{10}X_FX_A + a_{11}X_FX_M + a_{12}X_GX_S + a_{13}X_GX_P + a_{14}X_GX_A + a_{15}X_GX_M + a_{16}X_SX_P + a_{17}X_SX_A + a_{18}X_SX_M + a_{19}X_PX_A + a_{20}X_PX_M + a_{21}X_AX_M \quad (3)$$

Here,  $y$  represents the response variables  $T_{gs}$ ,  $K$ ,  $E$ ,  $B$ ,  $T'_g$ ,  $T'_m$ ,  $w'_s$ . Parameters  $a_1$ – $a_{21}$  are the coefficients from the regression model for the analysis of variance (ANOVA). A confidence level of 95% ( $p < 0.05$ ) with MODDE 7.0 statistical software (Umetrics AB) was used. Equation (3) was reduced to its corresponding pruned forms after the omission of the statistically nonsignificant coefficient values ( $p > 0.10$ ) and mathematical models were developed.

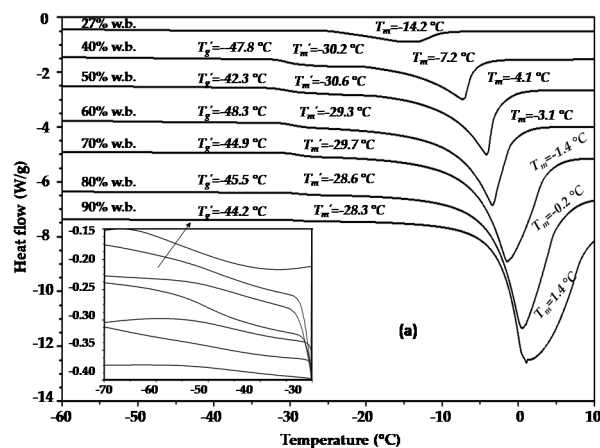
## 3. Results

### 3.1. DSC Thermograms

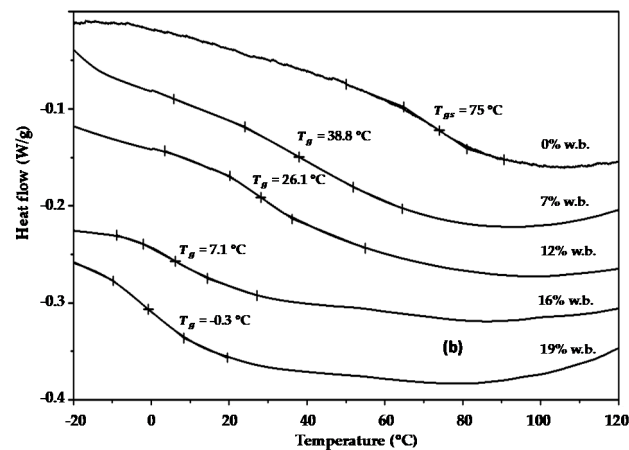
Figure 1a shows as an example the heating DSC thermograms obtained for the model food system with the chemical composition of  $0.45X_F:0.15X_P:0.4X_M$  (experiment no. 6, Table 1) and prepared with moisture contents in the range of 27% to 90% wet basis (w.b.).

The thermograms show three thermal events in which the endothermic peak of ice melting was the most visible feature, preceded by two changes in the baseline, both with characteristics typical of a glass transition [11]. It can be observed that the  $T_m$  value was greatly depressed as the solid content was increased, ranging in this case from 1.4 to  $-14.2$  °C. The melting point is defined as the temperature at which the liquid and solid phases of water at a given pressure are in equilibrium, while the presence of solutes increases the complexity of crystallization and reduces the partial pressure of water. Therefore, the equilibrium between the two phases (ice and water) can only be reached through a reduction in temperature [1,2,39]. It was also evident that the phase change peak becomes smaller as the solid content increases in the sample because of the reduction of the amount of freezable water in the samples. For aqueous sugar solutions, as in this case, it has been suggested that the first transition can be attributed to the glass transition of the maximally freeze-concentrated phase ( $T'_g$ ), and the second transition can be considered as the beginning of the melting of ice crystals ( $T'_m$ ) [40]. Figure 1a shows that the first transition was detected between  $-48.3$  and  $-42.3$  °C and the second one between  $-30.6$  and  $-28.3$  °C. Both parameters varied very little when the water content varied between 27% and 90%, as observed by Grajales-Lagunes et al. [4] and Ruiz-Cabrera et al. [22]. Therefore, the corresponding average values of  $T'_g$  and  $T'_m$  for each of the samples in Table 1 were estimated, reported, and subjected to statistical analysis using Equation (3), which are discussed later.

Figure 1b also shows as an example the reheating DSC thermograms obtained for the model food system with the chemical composition of  $0.45X_S:0.15X_P:0.4X_M$  (experiment no. 8, Table 1) and prepared in the reduced moisture range of 0% to 19% w.b. It can be observed that the samples with any moisture content exhibited a clear endothermic shift because of the glass transition, with  $T_g$  values ranging from  $-0.3$  °C to 75 °C. The  $T_g$  values became higher as the solid contents were increased in the samples because of the plasticizing effect of water on the glass transition temperature. It can also be seen in Figure 1b that glass transition occurred over a large temperature range (around 40 and 50 °C). These behaviors can be explained by the presence of maltodextrin in the samples. It is assumed that high molecular weight food components such as proteins, starches, and maltodextrin may exhibit glass transition with temperatures as high as 50 °C [2]. It is important to note, however, that good compatibility was achieved for the components, because global  $T_g$  values were observed in all the samples.



(a)



(b)

**Figure 1.** Differential scanning calorimetry (DSC) thermograms used for thermal analysis in model food systems: (a) the determination of  $T'_g$ ,  $T'_m$ , and  $T_m$  in experiment no. 6 ( $0.45X_F:0.15X_P:0.4X_M$ ) containing freezable water; (b) the determination of  $T_g$  in experiment no. 8 ( $0.45X_S:0.15X_P:0.4X_M$ ) containing unfreezable water.

The heating DSC thermograms of the aqueous model systems of exp. nos. 4, 19, 6, 22, and 5 (Table 1) were chosen to illustrate the effects of the maltodextrin concentration on the  $T'_g$ ,  $T'_m$ , and  $T_m$  values, as shown in Figure 2a. In this case, all the samples were prepared at the same moisture content of 60% w.b., whereas the maltodextrin mass fraction varied at intervals of approximately 0.2 in the concentration range of 0 to 0.8. As expected, the highest  $T_m$  value (0.8 °C) was obtained for the sample with the highest maltodextrin mass fraction (exp. no. 4), while the lowest  $T_m$  value (−6.6 °C) was obtained for the sample with no addition of maltodextrin (exp. no. 5). The freezing point depression is directly proportional to the molar concentration of a solution. This indicates that the lower the molecular mass of a solute, the higher the freezing point depression; that is, a high molecular weight substance has fewer molecules per gram than a low molecular weight one, which demonstrates fewer effects on the freezing point ( $T_m$ ). Therefore, the depression in the freezing point decreased as the amount of maltodextrin was increased, as shown in Figure 2a. The same trend was observed for the  $T'_m$  values, which varied from −9.4 °C to −38.6 °C. This trend is to be expected, since  $T'_m$  represents the end point of freezing or the beginning of the melting of ice crystals [40]. The values obtained for  $T'_g$ , however, which ranged from −46.2 to −54.5 °C, did not highlight a clear tendency as occurred with  $T_m$  and  $T'_m$  values. In the literature, it has been reported that  $T'_m$  and  $T'_g$  depend strongly on the type and molecular weight of the food components [2,40]. Therefore, this suggests that other factors such

as compound interactions are also involved. Note that only one transition at  $-9.4\text{ }^{\circ}\text{C}$  was observed for the sample of exp. no 4, and the value of  $T'_g$ , was not detected in this sample. These findings are similar to those of Flores-Ramírez et al. [11] and Roos and Karel [40], and are tentatively attributed to the overlapping of the glass transition with the ice melting caused by the HMW of maltodextrin.

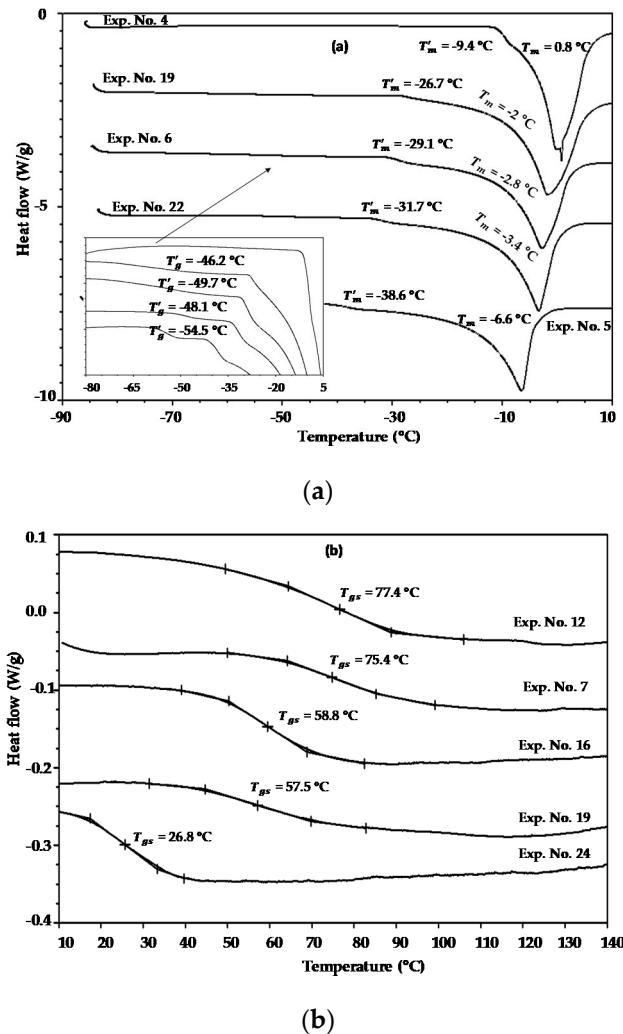


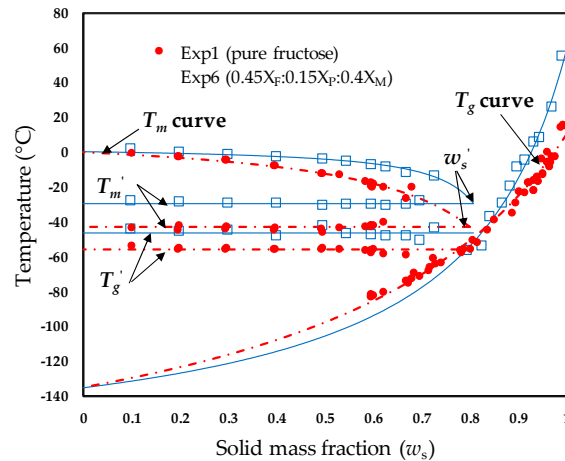
**Figure 2.** DSC thermograms used for thermal analysis in model food systems: (a) the effects of maltodextrin concentration on the  $T'_g$ ,  $T'_m$ , and  $T_m$  values of samples prepared at 60% w.b.; (b) the effects of maltodextrin concentration on the  $T_{gs}$  values of anhydrous samples.

Because water plays a strong role in the  $T_g$  of foods and its value is very low ( $-135\text{ }^{\circ}\text{C}$ ), not taking into account its effect, the reheating DSC thermograms of the model systems of exp. nos. 12, 7, 16, 19, and 24 (Table 1) equilibrated over Drierite<sup>®</sup> were chosen to understand the effects of maltodextrin addition on the glass transition temperatures of anhydrous samples ( $T_{gs}$ ), as shown in Figure 2b. In general, it can be established that all the model systems with added maltodextrin (exp. nos. 12, 7, 16, and 19) exhibited higher  $T_{gs}$  values than the model system without maltodextrin (exp. no. 24), which can be attributed to the high  $T_g$  value of the maltodextrin (170 to 180  $^{\circ}\text{C}$ ) [40]. No proportional relationship between  $T_g$  and the maltodextrin concentration was observed, however, because no significant difference between the  $T_g$  values was found for the anhydrous samples of exp. no. 12 and exp. no. 7, nor for the samples of exp. no. 16 and exp. no. 19 (Table 1). It is well established that the  $T_g$  values of amorphous materials are mainly affected by the molecular weight, chemical composition, and plasticizer [2,40]. Therefore, it is evident that the plasticizing effects of low molecular weight compounds such as glucose, fructose, and citric acid are also important in fruit juices [2].

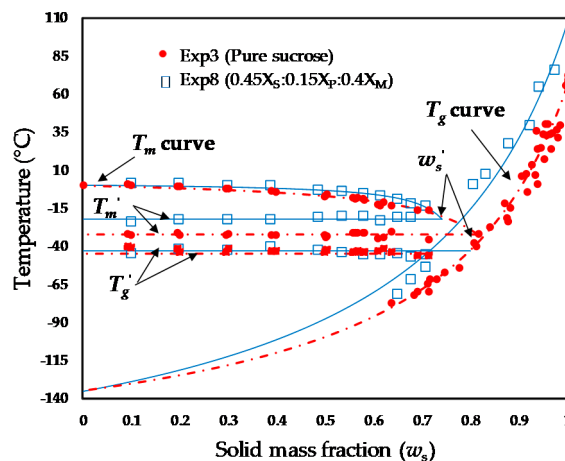


### 3.2. State Diagrams

The experimental freezing points and glass transition temperatures measured by DSC were plotted as functions of the solid contents ( $w_s$ ) in order to develop the state diagrams of each of the studied samples. As examples, a comparison of the state diagrams obtained for exp. no. 1 (pure fructose), exp. no. 6 ( $0.45X_F:0.15X_P:0.4X_M$ ), exp. no. 3 (pure sucrose), and exp. no. 8 ( $0.45X_S:0.15X_P:0.4X_M$ ) are respectively shown in Figure 3a,b.



(a)



(b)

**Figure 3.** Examples of state diagrams obtained for fruit juice model systems: (a) comparison of experiment no. 1 (pure fructose) and experiment no. 6 ( $0.45X_F:0.15X_P:0.4X_M$ ); (b) comparison of experiment no. 3 (pure sucrose) and experiment no. 8 ( $0.45X_S:0.15X_P:0.4X_M$ ).

As expected, a significant increase of the  $T'_g$ ,  $T'_m$ ,  $T_m$ , and  $T_g$  values was observed in the model food systems with added maltodextrin, and such effects can be better appreciated over the entire solid mass fraction scale, as shown in Figure 3. Generally, the predicted  $T_g$  curves with the G-T equation (Equation (1)) shifted upwards with increased maltodextrin content. In this way, the predicted  $T_{gs}$  values for pure fructose and pure sucrose were, respectively, 10.4 °C and 65.4 °C, whereas the corresponding values for the samples of exp. no. 6 and exp. o. 8, both with maltodextrin fractions of 0.4, were 60.3 °C and 107 °C, respectively (Table 2). The  $T_{gs}$  values estimated for fructose and sucrose were reasonably consistent with those reported in the literature for both sugars [2,41]. On the other hand, the predicted  $T_m$  curves with the Chen equation (Equation (2)) were less pronounced for the samples containing maltodextrin (exp. no. 6 and exp. no. 8), which always exhibited higher

$T_m$  values in the freezable water domain. As previously mentioned, the freezing point depression is highly dependent on the molecular weight of the systems. This reduced freezing point depression may be relevant for industrial processes such as subcooling, in which the partial or total formation of ice crystals is achieved at relatively high temperatures ( $-4\text{ }^\circ\text{C}$ ), and thus the availability of water and water activity to slow microorganism growth is reduced. From Figure 3, it is also observed that the added maltodextrin exhibits a greater influence on the  $T'_m$  values than the  $T'_g$  values, because  $T'_m$  represents the end freezing point, which is also highly dependent on the molecular weights of the compounds, as previously discussed. In Figure 3, it can also be verified that both  $T'_g$  and  $T'_m$  exhibited little variation from the solid mass fraction; therefore, average values can be considered in these samples [4,22]. As a general trend, a proportional increase of the maltodextrin concentration was expected for the  $w'_s$  values, because the unfreezable water mass fraction ( $w'_w = 1 - w'_s$ ) should be reduced as the solid content of maltodextrin is increased in the samples. Nevertheless, the opposite compositional dependence of  $w'_s$  has also been established for some samples, such as pure sucrose (Figure 3b, Table 2), which exhibited one of the highest values of  $w'_s$  (0.796 g solid/g sample). Therefore, an experimental method other than the intersection of the average value of  $T'_m$  with the  $T_m$  curve to accurately determine the maximum freeze concentration is required.

**Table 2.** Fitting parameters of Equations (1) and (2), and parameters of the maximal-freeze-concentration condition (MFCC).

Experiment Parameters of Equation (1)				Parameters of Equation (2)			MFCC		
No.	$T_{gs}$ ( $^\circ\text{C}$ )	$K$	$R^2$	$E$	$B$	$R^2$	$T'_g$ ( $^\circ\text{C}$ )	$T'_m$ ( $^\circ\text{C}$ )	$w'_s$
1	10.4	2.90	0.986	0.0954	0.1668	0.991	-55.9	-42.8	0.739
2	31.8	3.79	0.994	0.1103	0.0557	0.968	-55.7	-41.8	0.783
3	65.2	4.68	0.975	0.0584	0.0980	0.964	-43.1	-32.5	0.796
4	157.3	10.32	0.808	0.0085	0.1595	0.929	-9.5	-9.5	0.801
5	25.6	3.33	0.990	0.0781	0.2178	0.991	-56.4	-38.7	0.716
6	60.3	5.59	0.983	0.0371	0.1280	0.971	-46.6	-29.6	0.807
7	61.6	5.75	0.964	0.0535	0.0741	0.974	-54.8	-30.2	0.812
8	107	4.09	0.970	0.0256	0.2442	0.975	-44.6	-22.3	0.741
9	24.7	3.53	0.981	0.0877	0.0697	0.950	-50.2	-38.4	0.791
10	41	3.85	0.984	0.0786	0.1076	0.971	-52.0	-38.8	0.781
11	19.1	3.52	0.976	0.0956	0.0936	0.972	-54.6	-42.6	0.781
12	64	6.12	0.876	0.0517	0.1399	0.969	-52.0	-32.0	0.780
13	16.4	3.73	0.954	0.0734	0.1958	0.987	-56.9	-39.3	0.738
14	34.4	4.04	0.987	0.0806	0.1805	0.987	-57.1	-39.0	0.737
15	46.6	4.16	0.951	0.0673	0.1340	0.974	-50.4	-34.7	0.768
16	37.7	4.18	0.899	0.0706	0.1770	0.983	-55.9	-36.9	0.746
17	66	5.44	0.904	0.0552	0.1953	0.966	-51.6	-34.8	0.750
18	73.5	6.41	0.890	0.0553	0.2107	0.988	-52.3	-34.4	0.740
19	47.6	5.06	0.884	0.0385	0.0770	0.967	-47.4	-25.5	0.824
20	52.4	4.43	0.963	0.0529	0.2970	0.986	-55.5	-36.1	0.702
21	67.1	6.09	0.886	0.0700	0.1644	0.985	-55.4	-36.5	0.752
22	92.4	6.90	0.971	0.0408	0.2569	0.981	-48.9	-31.6	0.730
23	18.8	3.75	0.949	0.0841	0.1467	0.985	-56.4	-38.6	0.751
24	36.6	3.43	0.976	0.0583	0.2462	0.984	-53.5	-35.1	0.719
25	54.2	4.78	0.965	0.0801	0.0865	0.977	-55.8	-35.3	0.780

The estimated parameters of the G-T equation (Equation (1)), the Chen equation (Equation (2)), and the maximal-freeze-concentration condition for each of the studied samples are shown in Table 2. From Table 2, it is observed that for the model systems the parameter ranges are as follows:  $T_{gs}$ : 10.4  $^\circ\text{C}$ –157.3  $^\circ\text{C}$ ;  $K$ : 2.90–10.32;  $E$ : 0.0085–0.1103;  $B$ : 0.0557–0.297;  $T'_g$ : -57.1  $^\circ\text{C}$ –-9.5  $^\circ\text{C}$ ;  $T'_m$ : -42.8  $^\circ\text{C}$ –-9.5  $^\circ\text{C}$ ;  $w'_s$ : 0.702–0.824 g solid/g sample, with  $R^2$  values in the range 0.808–0.994. According to the data for several fruits, such as prickly pear cactus, orange, strawberry, pineapple, apple, date fruit,



raspberry, and blueberry, performed by Grajales-Lagunes et al. [4], these parameters varied as follows:  $T_{gs}$ : 12.2 °C–74.6 °C;  $K$ : 3.02–5.72;  $E$ : 0.0178–0.238;  $B$ : 0.04–0.1657;  $T'_g$ : –58.8 °C–46.4 °C;  $T'_m$ : –50.3 °C–31.2 °C;  $w'_s$ : 0.690–0.847. The upper limits for the  $T_{gs}$  and  $K$  parameters obtained in this study are well above those reported in the aforementioned study, while the lower limit of the  $E$  parameter is lower. Similarly, the upper limits of the  $T'_g$  and  $T'_m$  values are also well above the values reported for model and real systems [4]. These differences can be mainly attributed to the maltodextrin presence in the systems.

The obtained mathematical models, the ANOVA, and the effect of each component on the  $T_{gs}$ ,  $K$ ,  $E$ ,  $B$ ,  $T'_g$ ,  $T'_m$ , and  $w'_s$  values are given in Table 3. Equation (3) was used to interpret data variability with the determination coefficients, standard deviation, and coefficient of variation, respectively, in the ranges of 0.833–0.999, 0.00682–6.22, and 1.22–23.2. In addition, significance values varied between 0.2143 and <0.0001 (Table 3). From Table 3, it is observed that  $T_{gs}$ ,  $K$ ,  $E$ ,  $B$ ,  $T'_g$ ,  $T'_m$ , and  $w'_s$  were all linearly affected by the mass fractions of the components, followed by binary interactions, with the parameters  $T'_g$  and  $w'_s$  being the most affected. Taking into account the regression coefficients of the models, it can be seen that pectin ( $X_P$ ) and citric acid ( $X_A$ ) are the most important variables affecting all parameters, while the interactions of maltodextrin ( $X_M$ ) with the other components play important roles in the  $T'_m$  values, and the interactions of maltodextrin and pectin with other components have important effects on the parameter  $B$ . Regarding the ANOVA, it can be observed (Table 3) that all of the models are significant ( $P(F > F_0)$ ), with the exception of the parameter  $w'_s$ , and there is a high probability that other factors not included in the model (noise) affect this response variable. The high values obtained for  $R^2$  indicated that good control in the performance of the experiments and in the parameter determinations was achieved. On the other hand, the coefficients of variation shown in Table 3 generally indicated that there is homogeneity among the obtained data.

**Table 3.** Solute composition-based mathematical models and ANOVA ( $p < 0.05$ ).

Model	ANOVA			
	P (F > F <sub>0</sub> )	R <sup>2</sup>	S. D.	C.V. (%)
$T_{gs} = 8.31X_F + 29.98X_G + 58.68X_S + 1295.36X_P - 885.31X_A + 10.52X_M - 2139.92X_F X_P + 1653.18X_F X_A - 2555.95X_G X_P + 2109.04X_G X_A + 122.3X_G X_M - 3002.49X_S X_P + 2526.09X_S X_A + 468.11X_S X_M$	<0.0001	0.983	6.22	11.86
$K = 2.9X_F + 3.76X_G + 4.48X_S - 130.1X_P + 119.4X_A + 3.59X_M + 109.55X_F X_P - 106.31X_F X_A + 72.36X_G X_P - 67.19X_G X_A + 12.55X_G X_M + 28.65X_S X_M + 119.8X_P X_A + 249.97X_P X_M - 248.14X_A X_M$	<0.0001	0.984	0.31	6.42
$E = 0.946X_F + 0.1019X_G + 0.0617X_S + 0.0543X_P + 0.0648X_A - 0.0003 - 0.1471X_P X_P - 0.0719X_S X_M$	<0.0001	0.94	0.00682	10.61
$B = 0.1413X_F + 0.0645X_G + 0.0956X_S - 9.0225X_P + 3.9767X_A - 0.0164X_M + 8.3373X_F X_P + 8.0965X_G X_P + 7.8839X_S X_P + 1.0128X_S X_M + 14.3016X_P X_M - 9.8217X_A X_M$	0.0018	0.833	0.04	23.25
$T'_g = -55.95X_F - 55.56X_G - 43.16X_S - 2063.09X_P + 1103.46X_A - 34.36X_M + 4.43X_F X_G - 1.41X_F X_S + 2027.37X_F X_P - 1249.55X_F X_A - 23.35X_F X_M - 11.19X_G X_S + 1899.63X_G X_P - 1130.07X_G X_A - 22.25X_G X_M + 1921.26X_S X_P - 1169.78X_S X_A - 4.93X_S X_M + 1987.27X_P X_A + 2819.84X_P X_M - 2024.59X_A X_M$	<0.0001	0.999	0.61	1.2
$T'_m = -42.92X_F - 42.31X_G - 33.39X_S - 72.78X_P + 13.8X_A - 10.8X_M - 17.99X_F X_M - 21.09X_G X_M - 15.8X_S X_A + 134.61X_P X_M - 172.4X_A X_M$	<0.0001	0.994	0.69	2.02
$w'_s = 0.75X_F + 0.78X_G + 0.80X_S + 51.35X_P - 36.73X_A + 0.72X_M + 0.08X_F X_G + 0.03X_F X_S - 53.72X_F X_P + 39.01X_F X_A + 0.05X_F X_M + 0.02X_G X_S - 52.92X_G X_P + 38.22X_G X_A - 0.30X_G X_M - 53.85X_S X_P + 39.16X_S X_A - 0.40X_S X_M - 19.73X_P X_A - 65.01X_P X_M + 57.76X_A X_M$	0.2143	0.921	0.02	2.94

P (F > F<sub>0</sub>) = Fisher probability; S.D. = Standard deviation; C.V. = Coefficient of variation.

As an example, the performance of the empirical equations given in Table 3 can be observed in Figure 4, where a comparison between the predicted state diagrams at different maltodextrin mass fractions for the model food system 0.283X<sub>F</sub>:0.283X<sub>G</sub>:0.283X<sub>S</sub>:0.075X<sub>A</sub>:0.075X<sub>P</sub> (experiment no.5, Table 1) was performed. The solid composition of experiment no. 5. was chosen because sucrose, fructose, glucose, pectin, and citric acid are the main solutes of fruit and vegetables, and the maltodextrin mass fraction in the sample was varied between 0 and 0.6. In this case, it was found that the higher the value of the maltodextrin mass fraction ( $X_M$ ), the higher the values of  $T'_g$ ,  $T'_m$ , and  $w'_s$ , and the less pronounced the curvature of the  $T_m$  curve. On the other hand, although the curvatures of the predicted  $T_g$  curves of samples containing maltodextrin were more pronounced compared with the sample without maltodextrin, no significant differences between the  $T_g$  curves were found when maltodextrin mass fractions of 0.3 and 0.6 were used. A dominant role of the  $T_g$  of amorphous mango

pulp at a higher maltodextrin weight fraction than 0.7 was also observed by Fongin et al. [38]. Perhaps this is one of the reasons why high concentrations of maltodextrins are used as carrier agents in spray drying processes. In this context, the solute-composition-based mathematical models resulting from this study are relevant for predicting state diagrams to monitor the progress and development of various processes, such as freezing, refrigeration, and drying.

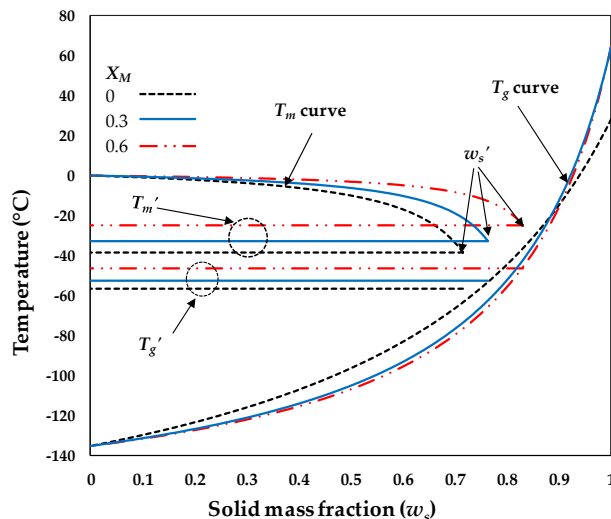


**Figure 4.** Influence of the maltodextrin mass fraction on the predicted state diagram for the fruit juice model system of experiment no. 5 using  $X_M = 0, 0.3$  and  $0.6$ .

#### 4. Conclusions

The effects of maltodextrin addition on  $T'_g$ ,  $T'_m$ ,  $T_m$ , and  $T_g$  during the construction of state diagrams of several fruit juice model systems were investigated. Increasing the maltodextrin mass fraction resulted in a significant increase of the abovementioned thermal transitions. Maltodextrin mass fractions higher than 0.4, however, are required to induce a significant increase of  $T'_g$ ,  $T'_m$ ,  $T_m$ , and  $T_g$  curves. Maltodextrin, therefore, can be considered as a good alternative in the formulation of cryoprotective media for adequate frozen preservation of high- and intermediate-moisture foodstuffs and as a carrier agent in the spray drying process. The developed mathematical models facilitated the determination of the influence of the chemical composition on the  $T_{gs}$ ,  $K$ ,  $E$ ,  $B$ ,  $T'_g$ ,  $T'_m$ , and  $w'_s$  values, and could also be used to predict the state diagrams of samples as a function of the concentrations of solutes predominant in fruit juices and the maltodextrin weight fraction. In this context, the solute-composition-based mathematical models resulting from this study are relevant to the design and optimization of processes and storage procedures for fruit products in the low-, intermediate-, and high-moisture domains.

**Author Contributions:** P.G.-C. contributed to the concept of the study and carried out the experiments. A.F.-R. and C.G.-H. assisted with DSC measurements and sample preparation. R.G.-G. contributed to the experimental design and data analysis. A.G.-L. and M.A.-A. contributed to the interpretation of the results and the preparation of the manuscript. M.A.R.-C. contributed to the concept, the interpretation of the results, and the preparation of the manuscript. All authors have read and agreed to the published version of the manuscript.

**Funding:** This research was funded by the Mexican National Council of Science and Technology (project CB2017-2018/A1-S-32348).

**Acknowledgments:** The authors acknowledge the financial support of the Mexican National Council of Science and Technology (CONACyT) with the project CB2017-2018/A1-S-32348 and the scholarship provided to P. García-Coronado (Grant No. 862541) for his MSc studies.

**Conflicts of Interest:** The authors declare no conflict of interest. The founding sponsors had no role in the design of the study, in the collection, analyses, or interpretation of data, in the writing of the manuscript, nor in the decision to publish the results.

## References

1. Rahman, M.S. Food stability determination by macro-micro region concept in the state diagram and by defining a critical temperature. *J. Food Eng.* **2010**, *99*, 402–416. [[CrossRef](#)]
2. Sablani, S.S.; Syamaladevi, R.M.; Swanson, B.G. A review of methods, data and applications of state diagrams of food systems. *Food Eng. Rev.* **2010**, *2*, 168–203. [[CrossRef](#)]
3. Buera, M.P.; Roos, Y.; Levine, H.; Slade, L.; Corti, H.R.; Reid, D.S.; Auffret, T.; Angell, C.A. State diagrams for improving processing and storage of foods, biological materials, and pharmaceuticals (IUPAC Technical Report). *Pure Appl. Chem.* **2011**, *83*, 1567–1617. [[CrossRef](#)]
4. Grajales-Lagunes, A.; Rivera-Bautista, C.; Loredó-García, I.O.; González-García, R.; González-Chávez, M.M.; Schmidt, S.J.; Ruiz-Cabrera, M.A. Using model food systems to develop mathematical models for construction of state diagrams of fruit products. *J. Food Eng.* **2018**, *230*, 72–81. [[CrossRef](#)]
5. Celli, G.B.; Ghanem, A.; Brooks, M.S.L. Influence of freezing process and frozen storage on the quality of fruits and fruit products. *Food Rev. Int.* **2016**, *32*, 280–304. [[CrossRef](#)]
6. Sagar, V.R.; Suresh Kumar, P. Recent advances in drying and dehydration of fruits and vegetables: A review. *J. Food Sci. Technol.* **2010**, *47*, 15–26. [[CrossRef](#)]
7. Soliva-Fortuny, R.C.; Martín-Belloso, O. New advances in extending the shelf life of fresh-cut fruits: A review. *Trends Food Sci. Technol.* **2003**, *14*, 341–353. [[CrossRef](#)]
8. Liu, D.K.; Xu, C.C.; Guo, C.X.; Zhang, X.X. Sub-zero temperature preservation of fruits and vegetables: A review. *J. Food Eng.* **2020**, *275*. [[CrossRef](#)]
9. Silva, C.L.M.; Goncalves, E.M.; Brandao, T.R.S. Freezing of fruits and vegetables. In *Frozen Food Science and Technology*; Evans, J.A., Ed.; Blackwell Publishing: Singapore, 2008; pp. 165–183.
10. Aschenbrenner, M.; Kulozik, U.; Foerst, P. In situ determination of the physical state of biological samples during freeze drying. *Dry. Technol.* **2011**, *29*, 461–471. [[CrossRef](#)]
11. Flores-Ramírez, A.J.; García-Coronado, P.; Grajales-Lagunes, A.; González-García, R.; Abud Archila, M.; Ruiz-Cabrera, M.A. Freeze-concentrated phase and state transition temperatures of mixtures of low and high molecular weight cryoprotectants. *Adv. Polym. Technol.* **2019**, 5341242. [[CrossRef](#)]
12. Liu, J. Physical characterization of pharmaceutical formulations in frozen and freeze-dried solid states: Techniques and applications in freeze-drying development. *Pharm. Dev. Technol.* **2006**, *11*, 3–28. [[CrossRef](#)]
13. Patel, S.M.; Nail, S.L.; Pikal, M.J.; Geidobler, R.; Winter, G.; Hawe, A.; Davagnino, J.; Gupta, S.R. Lyophilized drug product cake appearance: What is acceptable? *J. Pharm. Sci.* **2017**, *106*, 1706–1721. [[CrossRef](#)]
14. Singh, K.J.; Roos, Y.H. State transitions and freeze concentration in trehalose–protein–cornstarch mixtures. *LWT Food Sci. Technol.* **2006**, *39*, 930–938. [[CrossRef](#)]
15. Syamaladevi, R.M.; Manahiloh, K.N.; Muhunthan, B.; Sablani, S.S. Understanding the influence of state/phase transitions on ice recrystallization in atlantic salmon (*Salmo salar*) during frozen storage. *Food Biophys.* **2012**, *7*, 57–71. [[CrossRef](#)]
16. Bhandari, B.R.; Datta, N.; Howes, T. Problems associated with spray drying of sugar-rich foods. *Dry. Technol.* **1997**, *15*, 671–684. [[CrossRef](#)]
17. Bhandari, B.R.; Howes, T. Implication of glass transition for the drying and stability of dried foods. *J. Food Eng.* **1999**, *40*, 71–79. [[CrossRef](#)]
18. Al-Farsi, K.A.; Al-Habsi, N.A.; Rahman, M.S. State diagram of crystallized date-syrup: Freezing curve, glass transition, crystals-melting and maximal-freeze-concentration condition. *Thermochim. Acta* **2018**, *666*, 166–173. [[CrossRef](#)]
19. Bai, Y.; Rahman, M.S.; Perera, C.O.; Smith, B.; Melton, L.D. State diagram of apple slices: Glass transition and freezing curves. *Food Res. Int.* **2001**, *34*, 89–95. [[CrossRef](#)]
20. Fabra, M.J.; Talens, P.; Moraga, G.; Martínez-Navarrete, N. Sorption isotherm and state diagram of grapefruit as a tool to improve product processing and stability. *J. Food Eng.* **2009**, *93*, 52–58. [[CrossRef](#)]
21. Rahman, M.S. State diagram of date flesh using differential scanning calorimetry (DSC). *Int. J. Food Prop.* **2004**, *7*, 407–428. [[CrossRef](#)]
22. Ruiz-Cabrera, M.A.; Rivera-Bautista, C.; Grajales-Lagunes, A.; González-García, R.; Schmidt, S.J. State diagram for mixtures of low molecular weight carbohydrates. *J. Food Eng.* **2016**, *171*, 185–193. [[CrossRef](#)]
23. Syamaladevi, R.M.; Sablani, S.S.; Tang, J.; Powers, J.; Swanson, B.G. State diagram and water adsorption isotherm of raspberry (*Rubus idaeus*). *J. Food Eng.* **2009**, *91*, 460–467. [[CrossRef](#)]

24. Telis, V.R.N.; Sobral, P.J.A. Glass transitions and state diagram for freeze-dried pineapple. *Lebensm. Wiss. Technol.* **2001**, *34*, 199–205. [[CrossRef](#)]
25. Vasquez, C.; Díaz-Calderon, P.; Enrione, J.; Matiacevich, S. State diagram, sorption isotherm and color of blueberries as a function of water content. *Thermochim. Acta* **2013**, *570*, 8–15. [[CrossRef](#)]
26. Zhao, J.H.; Liu, F.; Wen, X.; Xiao, H.W.; Ni, Y.Y. State diagram for freeze-dried mango: Freezing curve, glass transition line and maximal-freeze-concentration condition. *J. Food Eng.* **2015**, *157*, 49–56. [[CrossRef](#)]
27. Verma, A.; Singh, S.V. Spray drying of fruit and vegetable juices: A review. *Crit. Rev. Food Sci. Nutr.* **2015**, *55*, 701–719. [[CrossRef](#)]
28. Maity, T.; Saxena, A.; Raju, P.S. Use of hydrocolloids as cryoprotectant for frozen foods. *Crit. Rev. Food Sci.* **2016**, *58*, 420–435. [[CrossRef](#)]
29. Joshi, A.J. A review and application of cryoprotectant: The science of cryonics. *PharmaTutor* **2016**, *4*, 12–18.
30. Jaya, S.; Das, H.G.; Mani, S. Optimization of maltodextrin and tricalcium phosphate for producing vacuum dried mango powder. *Int. J. Food Prop.* **2006**, *9*, 13–24. [[CrossRef](#)]
31. Ferrari, C.C.; Marconi-Germer, S.P.; Dutra-Alvim, I.; Zaratini-Vissotto, F.; De Aguirre, J.M. Influence of carrier agents on the physicochemical properties of blackberry powder produced by spray drying. *Int. J. Food Sci. Technol.* **2012**, *47*, 1237–1245. [[CrossRef](#)]
32. Harnkarnsujarit, N.; Nakajima, M.; Kawai, K.; Watanabe, M.; Suzuki, T. Thermal properties of freeze-concentrated sugar phosphate solutions. *Food Biophys.* **2014**, *9*, 213–218. [[CrossRef](#)]
33. Yousefi, S.; Emam-Djomeh, Z.; Mousavi, S.M. Effect of carrier type and spray drying on the physicochemical properties of powdered and reconstituted pomegranate juice (*Punica granatum* L.). *J. Food Sci. Technol.* **2011**, *48*, 677–684. [[CrossRef](#)]
34. Silva, M.A.; Sobral, P.J.A.; Kieckbusch, T.G. State diagrams of freeze-dried camu-camu (*Myrciaria dubia* (HBK) Mc Vaugh) pulp with and without maltodextrin addition. *J. Food Eng.* **2006**, *77*, 426–432. [[CrossRef](#)]
35. Fabra, M.J.; Márquez, E.; Castro, D.; Chiralt, A. Effect of maltodextrins in the water-content-water activity-glass transition relationships of noni (*Morinda citrifolia* L.) pulp powder. *J. Food Eng.* **2011**, *103*, 47–51. [[CrossRef](#)]
36. Chen, Q.; Bi, Y.; Bi, J.; Zhou, L.; Wu, X.; Zhou, M. Glass transition and state diagram for jujube powders with and without maltodextrin addition. *Food Bioprocess Technol.* **2017**, *10*, 1606–1614. [[CrossRef](#)]
37. Fongin, S.; Kawai, K.; Harnkarnsujarit, N.; Hagura, Y. Effects of water and maltodextrin on the glass transition temperature of freeze-dried mango pulp and an empirical model to predict plasticizing effect of water on dried fruits. *J. Food Eng.* **2017**, *210*, 91–97. [[CrossRef](#)]
38. Fongin, S.; Alvino Granados, A.E.; Harnkarnsujarit, N.; Hagura, Y.; Kawai, K. Effects of maltodextrin and pulp on the water sorption, glass transition, and caking properties of freeze-dried mango powder. *J. Food Eng.* **2019**, *247*, 95–103. [[CrossRef](#)]
39. Cornillon, P.; Andrieu, J.; Duplan, J.C.; Laurent, M. Use of nuclear magnetic resonance to model thermophysical properties of frozen and unfrozen model food gels. *J. Food Eng.* **1995**, *25*, 1–19. [[CrossRef](#)]
40. Roos, Y.; Karel, M. Water and molecular weight effects on glass transitions in amorphous carbohydrates and carbohydrate solutions. *J. Food Sci.* **1991**, *56*, 1676–1681. [[CrossRef](#)]
41. Vanhal, I.; Blond, G.J. Impact of melting conditions of sucrose on its glass transition temperature. *J. Agric. Food Chem.* **1999**, *47*, 4285–4290. [[CrossRef](#)]



## RESUMEN EN EXTENSO 3

Artículo enviado a la revista:

**International Journal of Food & Technology**



Effect of maltodextrin weight fraction on the amorphous state and critical storage conditions of freeze-dried juices

**Alma Flores-Ramírez, Alicia Grajales-Lagunes, Miguel Abud-Archila,  
Miguel A. Ruiz-Cabrera**

## INTRODUCCIÓN

Las frutas en polvo son uno de los productos más importantes en la industria alimentaria. Los procesos de deshidratación como el secado por aspersion, la liofilización, espumado combinado con convección y el secado por ventana refractante se utilizan generalmente para producir polvos a partir de jugos de fruta, los que generalmente se obtienen en estado amorfo (Fernández *et al.*, 2011). Los materiales amorfos exhiben un volumen libre, entropía y niveles de energía más altos que sus contrapartes cristalinas, por lo que tienen una mayor solubilidad aparente y tasas de disociación más rápidas (Einfalt *et al.*, 2013). Los polvos amorfos son sistemas en estado de no equilibrio y metaestable, tienen propiedades dependientes de la temperatura y la humedad mostrando una estabilidad física más baja en comparación con los polvos cristalinos. Como consecuencia los polvos de fruta son extremadamente higroscópicos y pueden sufrir una transición del estado vítreo al estado gomoso, promoviendo cambios físicos como apelmazamiento, colapso y cristalización de azúcares (Mosquera *et al.*, 2012). Debido a que los polvos de frutas tienen valores bajos de  $T_g$  estando muy por debajo de las temperaturas típicas de almacenamiento (Syamaladevi *et al.*, 2009). Los polímeros con alto peso molecular, de bajo costo y baja viscosidad a altas concentraciones de sólidos, tales como las maltodextrinas se han utilizado para elevar los valores de  $T_{gs}$  y en consecuencia la mejora de las condiciones de almacenamiento críticas de los polvos de frutas. García-Coronado *et al.* (2020), reportan que usando una fracción másica de maltodextrina DE 4-7( $X_{MD}$ ) se incrementan las propiedades térmicas de  $T_g'$ ,  $T_m'$  y  $T_g$ .

## OBJETIVOS

1. Evaluar el efecto de la fracción másica de maltodextrina con DE 4-7 ( $X_{MD}$ ) sobre las isothermas de sorción de agua y la transición vítrea de jugos liofilizados de tuna, kiwi, fresa y piña.
2. Determinar las condiciones críticas de almacenamiento de jugos liofilizados de tuna, kiwi, fresa y piña basados en los valores  $T_{gs}$ ,  $a_{WC}$   $X_{WC}$ .

## MATERIALES Y MÉTODOS

Cuatro frutas fueron elegidas para evaluar el efecto de la maltodextrina DE 4-7 sobre las condiciones de almacenamiento los sistemas reales. Para ello se obtuvieron los jugos de cada una de ellas (fresa, piña, kiwi y tuna). Los jugos se filtraron para eliminar los sólidos no solubles. Para conocer la composición de los sólidos solubles en los jugos de fruta se utilizó un HPLC Ultimate 3000 Thermo Scientific. Así mismo se le determinó los grados °Brix con un refractómetro digital Leica, para conocer el contenido de sólidos solubles totales. En base al contenido de sólidos se realizó un ajuste con la solución de maltodextrina al 40% y obtener fracciones másicas de 0, 0.4 y 0.8 de maltodextrina en los jugos de frutas. Posteriormente, las muestras fueron congeladas a una temperatura de - 80 °C durante 24 horas para favorecer la formación de pequeños cristales de hielo y liofilizadas a -63°C y 5 mTorr. Una vez obtenidos los diferentes polvos se procedió a llevarlos a un equilibrio de actividad de agua de 0 durante un período de 6 semanas. Después de este tiempo se almacenaron los jugos a diferentes actividades de agua (0.14-0.91) con soluciones de sales saturadas ( LiCl, CH<sub>3</sub>COOK, K<sub>2</sub>CO<sub>3</sub>, Mg (NO<sub>3</sub>)<sub>2</sub>, NaCl, KCl y BaCl<sub>2</sub>). Las diferentes muestras fueron pesadas cada 4 días hasta equilibrio constante. Después de este equilibrio se procedió a realizar el análisis calorimétrico de cada una de los jugos a las diferentes fracciones másicas y actividades de agua con la finalidad de determinar la temperatura de transición vítrea. La metodología calorimétrica consistió en dos calentamientos de la muestra el primero de ellos se llevó a cabo con la finalidad de fundir los cristales de los polvos y el segundo se realizó para determinar el valor de T<sub>g</sub>. Una vez obtenidos cada uno de estos parámetros se procedió a la modulación de la temperatura de transición vítrea mediante una ecuación polinómica y la modelación de la isoterma desorción mediante el modelo de GAB para así obtener los diagramas de estado simplificados para los jugos de piña fresa kiwi y tuna con y sin la adición de maltodextrina y conocer las condiciones críticas de almacenamiento.

## RESULTADOS

Dado que los solutos presentes en los jugos de fruta tienen una influencia sobre el valor de  $T_g$ , fue necesario conocer la concentración de glucosa, sacarosa, fructosa, ácido cítrico y pectina de cada jugo. Se encontró que el kiwi presenta mayor concentración de fructosa, la tuna presento concentraciones más altas de glucosa y la concentración más alta de sacarosa la presento el jugo de piña. Por otra parte, se obtuvieron los diagramas de estado que combinan la transición vítrea y las isoterms de sorción de jugos de frutas liofilizados adicionados con fracciones másicas de maltodextrina de 0, 0.4 y 0.8. El aumento gradual de  $X_w$  se atribuye al efecto predominante de las interacciones soluto-solvente y la disolución del soluto, mientras que la disminución de  $T_g$  se asocia con el efecto plastificante del agua. Los valores de  $T_g$  y  $X_w$  de los polvos que contenían maltodextrina, independientemente del valor de  $a_w$ , fue mayor que el de los polvos de jugo puros, este aumento fue mayor en los jugos de piña con maltodextrina, este aumento se pudo deber a la mayor presencia de sacarosa. Indicando que el aumento de  $a_{WC}$  y  $X_{WC}$  es dependiente de la composición de los jugos de fruta. Cuanto mayor sea el valor de  $X_{MD}$ , mayor será el efecto esperado sobre estas propiedades. Los jugos en polvo anhidros proporcionaron valores de  $T_{gs}$  que variaron de  $28.5 \pm 1.0$  a  $110.5 \pm 1.6$  °C, mientras que los valores mínimos se presentaron en los polvos de jugos naturales y los más altos en los polvos preparados con maltodextrina con  $X_{MD}$  de 0.8. Puede verse que  $a_{WC}$  y  $X_{WC}$  para el polvo de fresa variaron, de 0.078 a 0.590 y 0.024 a 0.137 (b. s.), para piña en polvo de 0,174 a 0,632 y de 0,029 a 0,142 (b. s.), para kiwi en polvo de 0,029 a 0,550 y de 0,013 a 0,129 (b. s.) y para tuna en polvo de 0,077 a 0,570 y de 0,017 a 0,120 (b. s.), respectivamente. Se encontró que los valores críticos de los polvos de jugo natural y los polvos que contienen maltodextrina de este estudio están en los rangos reportados en la literatura. Las características reveladas en los polvos almacenados a los diferentes actividades de agua son las siguientes: todos los polvos permanecieron inalterados por debajo de los valores de  $a_w$  correspondiente; se obtuvieron polvos en estado amorfo hasta una  $a_w$  de 0.52 con  $X_{MD}$  de 0.8; se



observó disolución de solutos y pardeamiento no enzimático en todas las muestras a  $a_w$  superiores a 0.75.

## CONCLUSIÓN

Los diagramas de estados de los polvos se describieron mediante modelos polinomiales y la ecuación de GAB. El aumento del valor de  $X_{MD}$  de 0 a 0,8 reportó un aumento significativo de los valores críticos. Los resultados también muestran que  $a_{wC}$  y  $X_{wC}$  de las muestras dependen del tipo de sólido presente en los jugos ( $p < 0.05$ ). Los valores críticos más altos se encontraron en los polvos de piña que van desde 0.174–0.632 y 0.029–0.142 (b. s.) y los más bajos en los jugos de kiwi en polvo, que van desde 0.029–0.550 y 0.013–0.129 (b. s.). Por encima de  $X_{MD}$  de 0,8, independientemente de la composición del jugo, todos los polvos tienden a tener el mismo valor de  $a_{wC}$ . Se demostró la idoneidad de  $a_{wC}$  definido con  $a_{wC}$  experimental para predecir la estabilidad de los polvos a 25 °C. Además, a 25 °C, todos los polvos preparados con  $X_{MD}$  de 0,8 fueron amorfos y estables hasta un  $a_{wC}$  de 0.52.

## BIBLIOGRAFÍA

1. Einfalt, T., Planinšek, O. & Hrovat, K. (2013). Methods of amorphization and investigation of the amorphous state. *Acta Pharmaceutica*, 63, 305–334.
2. Fernandes, F. A. N., Rodrigues, S., Law C. L. & Mujumdar, A. S. (2011). Drying of exotic tropical fruits: A comprehensive review. *Food and Bioprocess Technology*, 4, 163-185.
3. García-Coronado, P., Flores-Ramírez, A., Grajales-Lagunes, A., Godínez-Hernández, C., Abud-Archila, M., González-García, R., & Ruiz-Cabrera, M. A. (2020). The Influence of Maltodextrin on the Thermal Transitions and State Diagrams of Fruit Juice Model Systems. *Polymers*, 12(9), 2077.
4. Mosquera, L. H., Moraga, G. & Martínez-Navarrete, N. (2012). Critical water activity and critical water content of freeze-dried strawberry powder as affected by maltodextrin and arabic gum. *Food Research International*, 47, 201–206.

5. Syamaladevi, R. M., Sablani, S. S., Tang J., Powers, J. & Swanson, B. G. (2009). State diagram and water adsorption isotherm of raspberry (*Rubus idaeus*). *Journal of Food Engineering*, 91, 460–467

# RESUMEN GRÁFICO 3

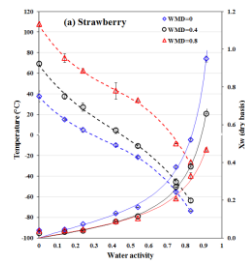
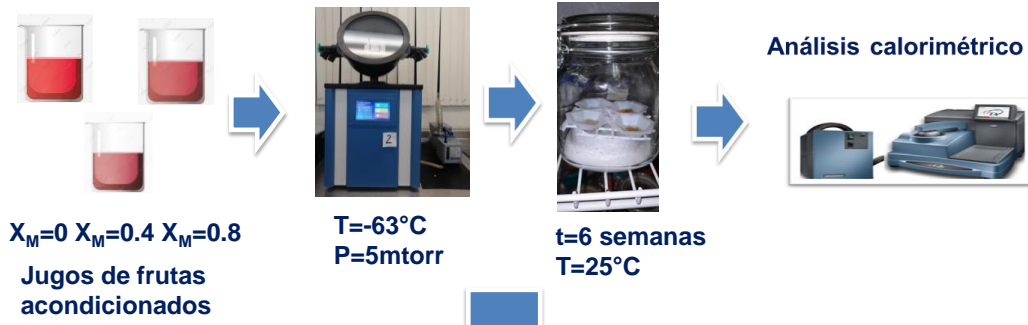
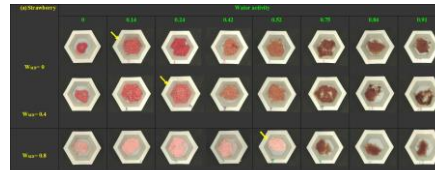


Diagrama de estado



Condiciones críticas de almacenamiento

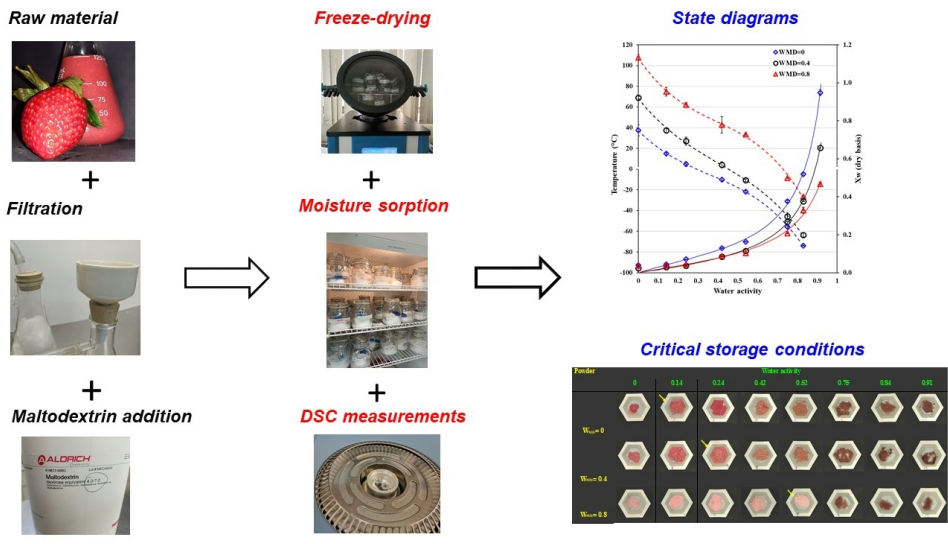


### Effect of maltodextrin weight fraction on the amorphous state and critical storage conditions of freeze-dried juices

Journal:	<i>International Journal of Food Science and Technology</i>
Manuscript ID	Draft
Manuscript Type:	Original Article
Date Submitted by the Author:	n/a
Complete List of Authors:	Flores-Ramírez, Alma; Universidad Autónoma de San Luis Potosí GRAJALES LAGUNES, Alicia; Universidad Autonoma de San Luis Potosi, Facultad de Ciencias Quimicas Abud Archila , Miguel ; Instituto Tecnológico de Tuxtla Gutiérrez RUIZ CABRERA, Miguel; Universidad Autonoma de San Luis Potosi, Facultad de Ciencias Quimicas
Keywords:	State diagram, fruit juice powders, glass transition, maltodextrin, storage stability

SCHOLARONE™  
Manuscripts

1  
2  
3  
4  
5  
6  
7  
8  
9  
10  
11  
12  
13  
14  
15  
16  
17  
18  
19  
20  
21  
22  
23  
24  
25  
26  
27  
28  
29  
30  
31  
32  
33  
34  
35  
36  
37  
38  
39  
40  
41  
42  
43  
44  
45  
46  
47  
48  
49  
50  
51  
52  
53  
54  
55  
56  
57  
58  
59  
60



355x200mm (96 x 96 DPI)

1  
2  
3  
4 1 **Effect of maltodextrin weight fraction on the amorphous state and critical**  
5  
6 2 **storage conditions of freeze-dried juices**  
7  
8  
9 3

10  
11 4 **Alma Flores-Ramírez<sup>1</sup>, Alicia Grajales-Lagunes<sup>1</sup>, Miguel Abud-Archila<sup>2</sup>, Miguel A. Ruiz-**  
12  
13 5 **Cabrera<sup>1,\*</sup>**

14  
15 6 1 Faculty of Chemical Science. University of San Luis Potosí. 6 Dr Manuel Nava Avenue, University Area,  
16  
17 San Luis Potosí, 78210, Mexico.  
18

19  
20 8 2 National Institute of Technology of Mexico. Technological Institute of Tuxtla Gutiérrez. Street km 1080,  
21  
22 9 Tuxtla Gutiérrez, 29050, Mexico.  
23

24 10 \*Corresponding author e-mail: [mruiz@uaslp.mx](mailto:mruiz@uaslp.mx)  
25  
26  
27  
28  
29  
30  
31  
32  
33  
34  
35  
36  
37  
38  
39  
40  
41  
42  
43  
44  
45  
46  
47  
48  
49  
50  
51  
52  
53  
54  
55  
56  
57  
58  
59  
60

## 21 **Summary**

22 State diagrams relating to water activity ( $a_w$ ), equilibrium moisture content ( $X_w$ ), and glass  
23 transition temperature ( $T_g$ ) are valuable tools for predicting amorphous fruit powders' storage  
24 procedure and stability. Thus, state diagrams were constructed to characterise the amorphous state  
25 and define the critical values of water content ( $X_{wc}$ ) and water activity ( $a_{wc}$ ) of freeze-dried juices  
26 of strawberry, pineapple, kiwi and prickly pear prepared with maltodextrin at the dry mass fraction  
27 ( $W_{MD}$ ) of 0, 0.4 and 0.8.  $T_g$  and sorption data were fitted with a polynomial equation and the GAB  
28 model, respectively ( $R^2 > 0.982$ ). A Tukey test was performed to evaluate the difference between  
29 critical values of the powders ( $p < 0.05$ ). The  $a_{wc}$  and  $X_{wc}$  increase with  $W_{MD}$  and depend on the  
30 solid types of juices. The highest critical values were found in pineapple powders, ranging from  
31 0.174 to 0.632 and 0.029 to 0.142 (dry basis), and the lowest ones in kiwi juice powders ranging  
32 from 0.029 to 0.550 and 0.013 to 0.129 (dry basis). For  $W_{MD}$  of 0.8, however, regardless of juice  
33 composition, stable powders in an amorphous state were obtained up to an  $a_w$  of 0.52 at 25°C.

34  
35 **Keywords:** state diagrams, fruit juice powders, glass transition, maltodextrin, storage stability

## CONCLUSIONES GENERALES

- 1 Los valores de  $T_g'$ ,  $T_m'$  y  $T_m$  aumentaron con respecto al peso molecular de crioprotector. El análisis estadístico de los datos ( $p < 0.05$ ) demostró que tanto la composición del soluto como del agua deben considerarse en la formulación de medios crioprotectores, ya que afectan significativamente los valores de  $T_g'$ ,  $T_m'$  y  $T_m$  ( $p < 0.05$ ).
- 2 Expresiones matemáticas para  $T_g'$ ,  $T_m'$  y  $T_m$  en función de las fracciones másicas de crioprotectores y agua y sus interacciones se desarrollaron para guiar la formulación de medios crioprotectores que involucran mezclas de más de dos crioprotectores para mejorar la estabilidad de almacenamiento y la calidad de productos alimenticios congelados con contenidos de humedad altos e intermedios con modificables formulaciones, como helados, purés, mermeladas, surimi, etc.
- 3 Se requieren fracciones másicas de maltodextrina superiores a 0.4 para inducir un aumento significativo de las curvas de  $T_g'$ ,  $T_m'$ ,  $T_m$  y  $T_g$ . Considerándose a la maltodextrina como alternativa en la formulación de medios crioprotectores para la adecuada conservación en congelado de productos alimenticios de humedad alta e intermedia y como agente acarreador en el proceso de secado por aspersion.
- 4 El desarrollo de modelos matemáticos facilitó la determinación de la influencia de la composición química en los valores de  $T_g$ ,  $K$ ,  $B$ ,  $T_g$ ,  $T_m'$  y  $x_{w,}'$  pudiendo predecir los diagramas de estado de muestras en función de las concentraciones de los solutos predominantes en jugos de frutas y la fracción de pesos de maltodextrina (DE 4-7).
- 5 La adición de fracciones másicas de maltodextrina (DE 4-7) de 0.4 o de 0.8 b.s a sistemas reales liofilizados (jugos de piña, fresa, tuna y kiwi) aumentan significativamente los valores de  $a_{wc}$ . La composición química de los polvos influye sobre los valores críticos, ya que la piña al contener mayor proporción de sacarosa en su composición presentó mayores valores de  $a_{wc}$  a una fracción másica de maltodextrina (DE 4-7) de 0.4. En fracciones másicas de 0.8 independiente de la composición todos los jugos presentan valores muy similares.